UNIVERSITÀ DEL PIEMONTE ORIENTALE

SCHOOL OF MEDICINE

DEPARTMENT OF HEALTH SCIENCE

Master's Degree in Medical Biotechnologies

President: Prof. Gianluca GAIDANO

Final Relation

RETROSPECTIVE STUDY BY MOLECULAR TECHNIQUES IN A CASE SERIES OF LONG-TERM SURVIVORS WITH GLIOBLASTOMA OF THE CENTRAL NERVOUS SYSTEM

Relator:

Chiar.mo Prof. Renzo Luciano BOLDORINI

Firmato digitalmente da Renzo Luciano Boldorini
Data: 02.07.2024 10:18:20 CEST
Organizzazione: UNIVERSITA' DEGLI STUDI DEL PIEMONTE ORIENTALE/01943490027

Candidate:

PRISCILLA BERNARDI

Matricula: 20006702

Summer Session

Academic year 2023/2024

INDEX

SUMMARY

Rational of the study: Glioblastomas (GBMs) are the most common and the deadliest primary malignant brain tumor. Despite modern therapies, it is still fatal with a very poor prognosis (median survival of 14 months). Due to short life expectancy, long survivors are defined as patients who live longer than two years post-diagnosis. The main goal of this study was to molecularly characterize a retrospective cohort of 19 patients with a diagnosis of IDH-wildtype glioblastoma and a survival equal to or greater than 25 months, in order to identify specific genetic and molecular alterations that may be correlated with the favorable prognosis observed in this subset of patients.

Planning of the study: Out of 332 patients diagnosed with glioblastoma (WHO 2021 or earlier) between 2013 and 2022 at the "AOU Maggiore della Carità" in Novara, only 19 were confirmed in the study due to meeting all the inclusion criteria: IDH-wildtype status, surviving ≥ 25 months, macroscopically radical resection and documented follow-up. An integrated analysis of molecular biomarkers was performed on all these samples, including the identification of hotspot mutations in the IDH1, IDH2, pTERT, H3F3A and HIST1H3B genes using Sanger Sequencing, evaluation of the methylation status of the MGMT promoter, determination of microsatellite instability, exploration of a multigene panel using Next-Generation Sequencing (NGS) and evaluation of the immunohistochemical expression of p53 and ATRX proteins.

Results: Regarding immunohistochemical investigations, 13/19 (68%) were found to be immunonegative for p53 and 5 (26%) immunopositive. 1 sample showed no immunoreactivity (<10%). All tumors maintained ATRX protein expression.
Regarding molecular investigations, pTERT was WT in 6 samples (40%) and mutated in 9 samples (60%) (2/9 had the C228T mutation and 7/9 had the C250T mutation) of the 15 evaluable samples. The H3F3A and HIST1H3B genes resulted WT in all the evaluable samples. 17/19 (89%) showed MSS and only 2 samples (11%) showed MSI-L. Regarding NGS results, the most frequently mutated genes among the 18 adequate samples were EGFR (33%), TP53 (22%), and PTEN (22%). Many samples showed amplification of EGFR (10, 55%) and FGFR3 (11, 61%). Additionally, 9 samples (50%) exhibited deletion of CDKN2A.
The survival analysis performed with Kaplan-Meier curves, showed a statistically significant difference (p<0,05) only for FGFR3 amplification (OS of non-amplified FGFR3 > OS of amplified FGFR3), stratified by patients with survival of <40 months and >40 months.

Conclusions: Although none of these factors alone appear sufficient to confer better clinical outcome, this work open the possibility to identify new therapeutical targets. This study showed a better survival in patients without amplification of FGFR3. This result should be considered as preliminary due to the low number of analyzed patients, but it put a focus on the possibility of finding new potentially druggable markers.
A subsequent full molecular characterization of large cohorts of long survival patients will be necessary to better understand the complex biology and cancerogenic pathways of glioblastoma and to disclose better therapeutic design.

1. INTRODUCTION

1.1 Epidemiology of Central Nervous System Tumors

Primary tumors of the Central Nervous System (CNS) are relatively rare compared to other solid tumors and globally represent 1.6% of new cancer diagnoses in 2020 and 2.5% of cancer-related deaths in the same year [1].

According to the Central Brain Tumor Registry of the United States (CBTRUS), the average annual age-adjusted incidence rate (AAAIR) of all malignant and non-malignant CNS tumors was 24.83 per 100,000 population between 2016 and 2020.

Approximately 27.9% of all CNS tumors were malignant and 72.1% were non-malignant [2]. **(Fig. 1)**

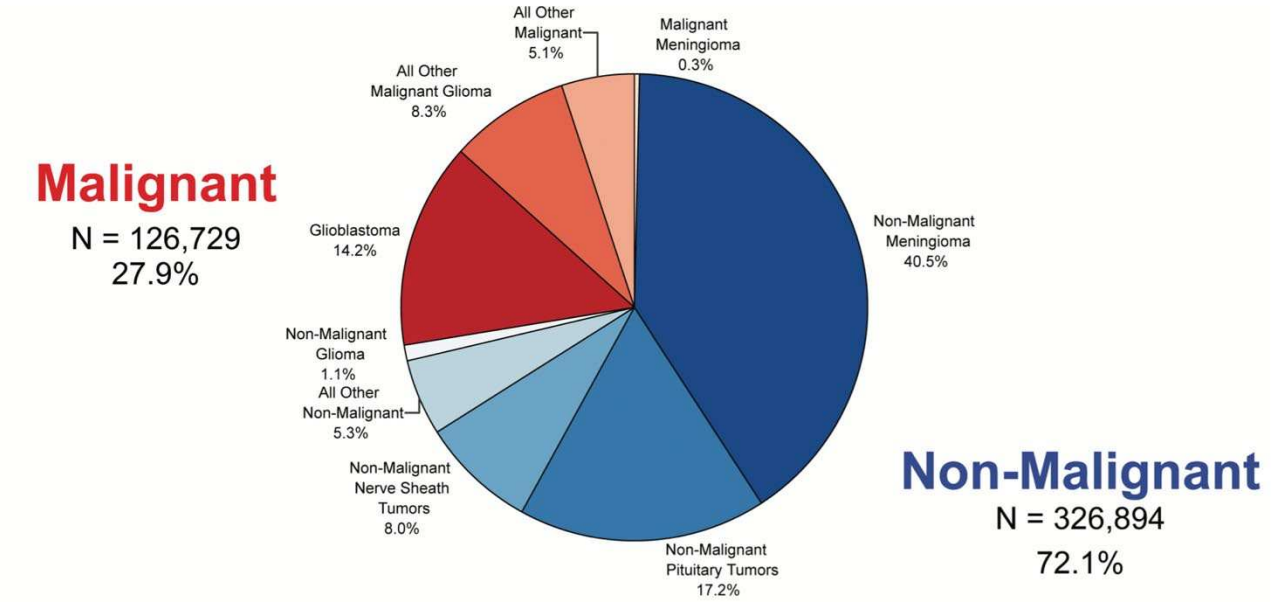

Fig. 1 Distribution of Primary Brain and Other Central Nervous System Tumors malignant and non-malignant.

It was estimated that 1,323,121 individuals lived with a previously diagnosed primary brain and other CNS tumor (malignant and non-malignant) in 2019.

In Italy in 2022, approximately 6,300 new diagnoses of CNS tumors were estimated, including 3,600 men and 2,700 women, with a prevalence of 52,800 patients, including 23,500 men and 29,300 women [3].

There is considerable variability in different geographic areas: the regions with a higher incidence are predominantly located in Europe, Southern Europe had the highest incidence, followed by Western Europe and Northern Europe. The lowest incidence was found in Middle Africa [4].

Human Development Index (HDI) seemed to be positively correlated with incidence of CNS cancer as the populations with very high HDI had the highest incidence and viceversa.

The effect of gender on the incidence was largely consistent throughout different geographical regions with males having an incidence rate of about 30% higher than females (4).

Gliomas accounted for 26.3% of all tumors. The most commonly occurring malignant brain and other CNS tumor histopathology was glioblastoma (14.2% of all tumors and 50.9% of all malignant tumors). Glioblastoma accounted for the majority of gliomas (60.2%). **(Fig.2)**

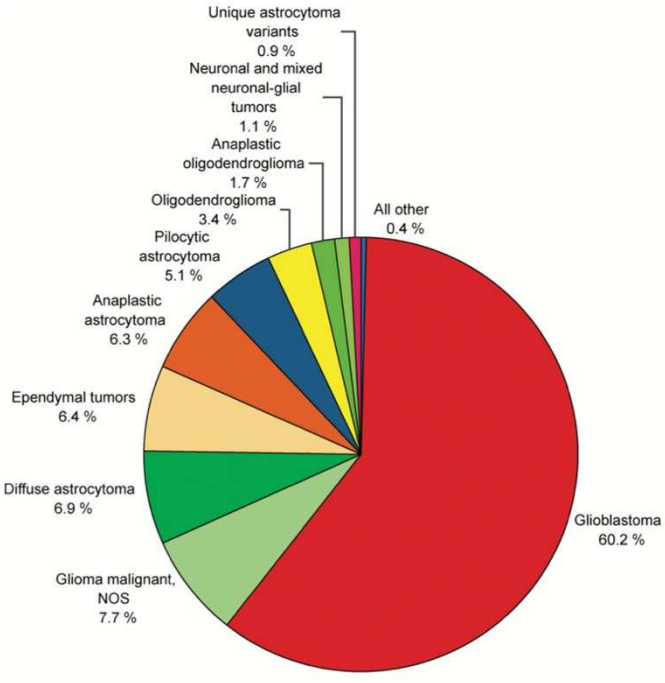

Fig. 2 Distribution of Primary Brain and Other Central Nervous System Gliomas by Histopathology subtypes.

The 5-year relative survival rate of a malignant CNS tumor was 35.7%, with minimal differences between females and males, with the former having a better prognosis.

However, there is significant variability depending on histology; the 5-year survival rate ranges from 94.6% for pilocytic astrocytomas to 6.7% for glioblastomas [3].

1.2 The WHO Classification of Gliomas

Diffuse gliomas are the most common primary brain tumors, with a clinical course that remains inevitably fatal for the majority of cases.

The 2016 WHO Classification of CNS Tumors integrated, for the first time, histopathological characteristics with molecular features. The 2016 edition added newly recognized neoplasms, and has deleted some entities, variants and patterns that no longer have diagnostic and/or biological relevance. The first molecular marker historically introduced was IDH (isocitrate dehydrogenase) mutation. Assessment of the mutational status of IDH1 and IDH2 allowed the classification of diffuse gliomas into IDH-mutant and IDH-wildtype, further subdivided into their respective four grades based on classic histological parameters. Additional molecular characterization has focused on the analysis of ATRX and TP53 genes, and co-deletion of the 1p/19q loci, which is necessary for the diagnosis of oligodendroglioma [5]. **(Fig. 3)**

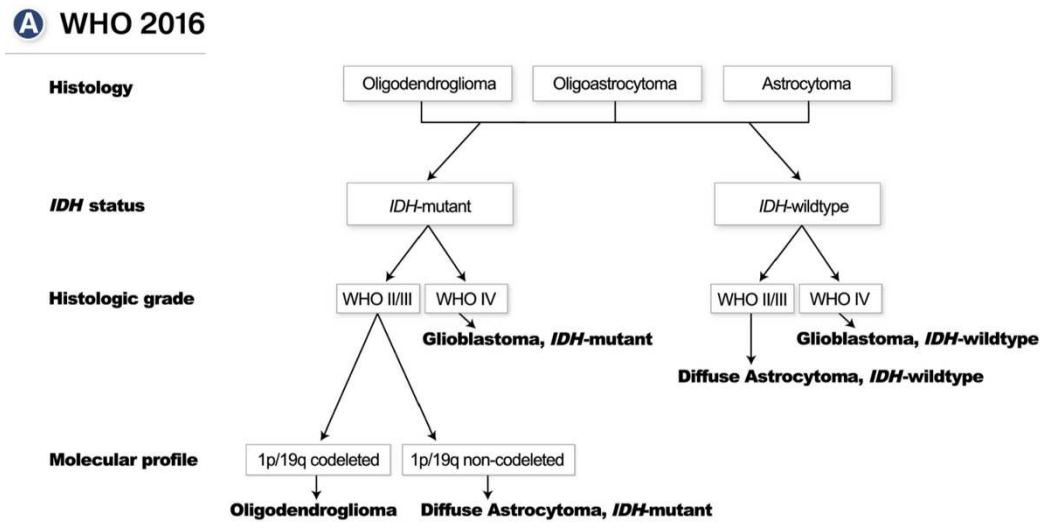

Fig. 3 WHO 2016 classification algorithm for central nervous system tumors.

The 2021 WHO Classification incorporates additional insights from genomic studies, bringing several changes to diagnostic principles and the nomenclature of diffuse gliomas, with significant implications for clinical practice. Clinically impactful changes include the addition of molecular criteria for the diagnosis of glioblastoma, IDH-wildtype, or astrocytoma, IDH-mutant, grade 4, even in the absence of histopathologic high-grade features [6].

In addition, the 2021 WHO classification has moved from Roman numerals (I, II, III, IV) to Arabic numerals (1, 2, 3, 4) for denoting tumor grades. **(Fig. 4)**

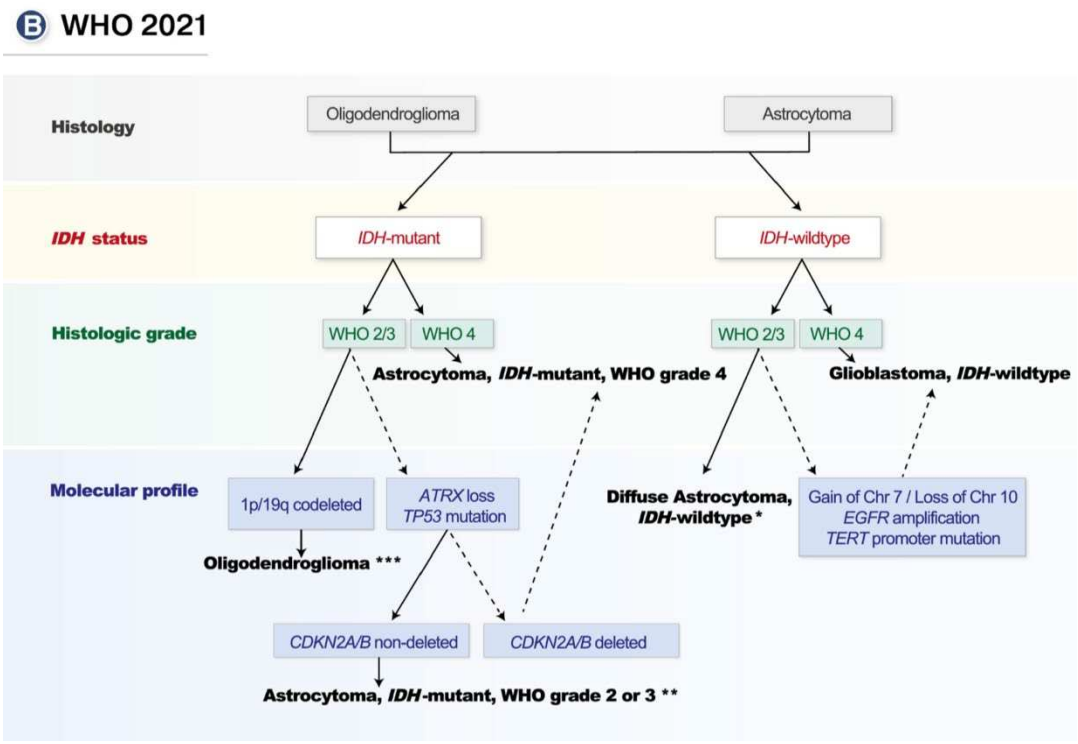

Fig. 4 WHO 2021 classification algorithm for central nervous system tumors.

The updated subcategories of diffuse adult gliomas are as follows:

- Astrocytoma, IDH-mutant;
- Oligodendroglioma, IDH-mutant and 1p/19q codeleted;
- Glioblastoma, IDH-wildtype.

IDH-mutant astrocytoma is classified directly as Grade IV when it exhibits one of the following characteristics:

- Histopathologically, the presence of microvascular proliferation or necrosis;

- Molecularly, homozygous deletion of the CDKN2A/B gene encoding tumor suppressors p16 and p14ARF [7].

The diagnosis of oligodendroglioma is based on the presence of an IDH-mutant glioma with 1p/19q codeletion. Grading depends on the presence of cellular or nuclear atypia and mitotic figures, similar to Grade II-III IDH-mutant astrocytomas [7].
The diagnosis of IDH-wildtype glioblastoma is based on the presence of an astrocytic glioma with IDH-wildtype and at least one of the following characteristics:

- Histopathologically, the presence of microvascular proliferation or necrosis;
- Molecularly, mutation of the TERT gene promoter, amplification of the EGFR gene, or concurrent gain of an additional chromosome 7 and complete deletion of chromosome 10 [7].

If a glioma is IDH-wildtype and does not exhibit histological or molecular features characteristic of glioblastoma, other types of tumors should be considered (e.g., diffuse pediatric gliomas, circumscribed gliomas, glioneuronal tumors, ependymomas). Additional molecular evaluations are necessary for accurate classification [8].

1.3 Risk factors

The identification of risk factors for the onset of gliomas could be extremely useful for the purposes of early diagnosis and prevention, but to date, data available in this regard are controversial, with only few accepted and confirmed risk factors.
Regarding genetic risk factors, most gliomas develop without a family history, but a small percentage can be classified as familial. The Li-Fraumeni syndrome, Turcot syndrome, and neurofibromatosis type 1 disorders are known to be associated with the highest risk of developing gliomas [9].
Recent genome-wide association studies (GWAS) have provided unambiguous evidence for common genetic susceptibility to gliomas, identified single nucleotide polymorphisms (SNPs) in different genes such as TERT, EGFR and CDKN2A/CDKN2B associated with risk. However, it is unclear how much of glioma heritability is attributable to common variation explained by these risk SNPs [10].

Regarding non-genetic risk factors, moderate or high exposure to ionizing radiation is the only ascertained environmental risk factor for the onset of gliomas, yet only represented by a small percentage of patients. The carcinogenic effect of ionizing radiation with an associated increased risk of gliomas development was assessed to be more present in children than in adults. Some studies evaluated the relationship between the intensity of radiation received in childhood and the subsequent development of CNS tumors and all of them agree that the risk of developing a brain tumor increases with the amount of radiation administered and the younger the age of the patients receiving radiotherapy [10].

1.4 Glioblastoma

Glioblastomas (GBMs) are the most common primary malignant brain tumor and the deadliest among patients with primary brain tumors. The overall age-adjusted incidence of glioblastoma in the United States is 3.26/100 000 people and increases with advanced age at diagnosis and male sex. Glioblastomas contribute disproportionately to morbidity and mortality, with a 5-year overall relative survival of only 6.9%, which varies by age at diagnosis and by sex [2].

Surgery, if feasible, followed by radiotherapy in combination with temozolomide chemotherapy (STUPP therapy) constitute the standard of care for the majority of patients with newly diagnosed glioblastoma [11].

Glioblastomas are thought to arise from neuroglial stem or progenitor cells and are characterized by molecular heterogeneity. Molecular profiling has identified genes and core pathways that are commonly mutated in sporadic glioblastoma. They present somatic molecular defects in 3 major processes: initiating tumor growth, evading senescence and enabling immortal growth. Genomic abnormalities in each of the 3 processes appear required for gliomagenesis. Some studies identified 3 main glioblastoma subgroups, each enriched for specific somatic alterations but the utility of molecular classification of glioblastoma into distinct subtypes remains unclear. None of the glioblastoma subtypes are predictive for treatment response to current therapies, and assignment of glioblastoma subtype can be challenging in some tumors

due to apparent coexistence of multiple subtypes within the same tumor and subtype "switching" through the course of the disease [12]. **(Fig. 5)**

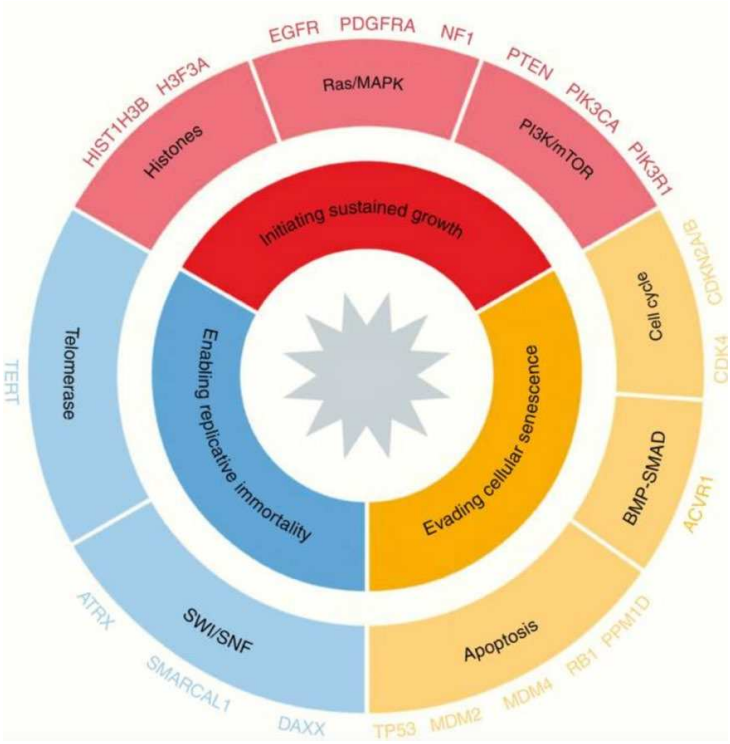

Fig. 5 Most frequently altered genes and pathways involved in gliomagenesis.

According to the latest WHO Classification of CNS tumors, glioblastoma is classified as glioblastoma, IDH wild-type, and requires an integrated histological and molecular diagnosis [6].

1.4.1 Histopathology

Glioblastoma is defined as a diffuse glioma, characterized by a high aptitude to infiltrate the surrounding brain tissue [13]. Most GBMs exhibit nuclear atypia, greater cellularity, multiple mitotic figures, and a high degree of nuclear pleomorphism. Microvascular proliferation is the major histological feature of high-grade gliomas, especially in GBMs, and consists on multilayered small-caliber blood vessels to indicate that they grow rapidly.

Necrosis is another important histological feature in GBM. Necrosis in GBM can present different morphologies: the most frequent is the so-called "Pseudopalisading", where

tumor cells are arranged radially in a picket fence-like distribution around a central area of necrosis [14]. **(Fig. 6)**

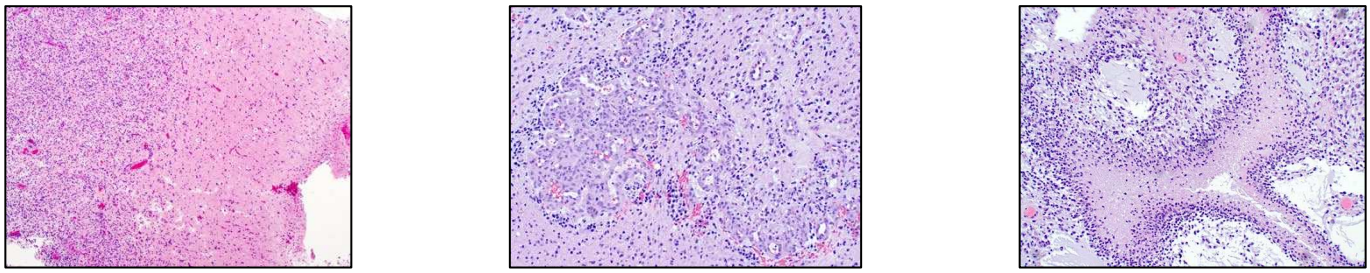

Hypercellular neoplasm with infiltration into surrounding brain parenchyma

Glomeruloid microvascular proliferation

Pseudopalisading necrosis with neoplastic cells surrounding areas of central necrosis

Fig. 6 Typical histopathological features of glioblastoma:
high cellular density, microvascular proliferation, palisading necrosis [15].

According to the WHO Classification of Tumors of the Central Nervous System (WHO 2021), IDH-wildtype glioblastoma can present three rare histological variants:

- Giant cell glioblastoma
- Gliosarcoma
- Epithelioid glioblastoma

Giant cell glioblastoma is histologically characterized by numerous large, bizarre giant cells, which have multiple nuclei and atypical mitosis, small fusiform syncytial cells, and a reticulin background (14). TP53 mutations are often observed, whereas mutations of IDH and TERT promoter (TERTp) are uncommon [16]. **(Fig. 7)**

Gliosarcomas are a special subtype of GBM with a biphasic component, which can either present glial or spindled sarcoma's morphology [14]. DNA copy number losses were frequent and amplifications were infrequent in gliosarcoma. The majority of copy number loss occurred on chromosomes 9 and 10, involving regions containing CDKN2A and CDKN2B genes [17]. **(Fig. 7)**

Epithelioid glioblastomas are dominated by a relatively uniform population of discohesive rounded epithelioid cells with eccentric nuclei and abundant eosinophilic cytoplasm, distinct cell membrane, paucity of cytoplasmic processes, and laterally positioned nucleus.

It's often associated with mutations in the BRAF gene, particularly the BRAF V600E mutation [14]. **(Fig. 7)**

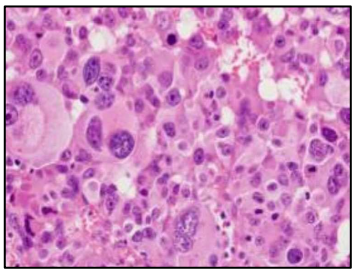

Giant cell glioblastoma (14)

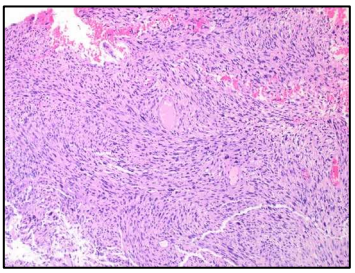

Gliosarcoma (18)

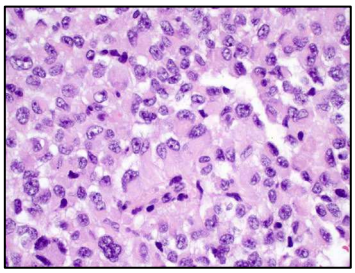

Epithelioid glioblastoma (15)

Fig. 7 Histological subtypes of glioblastoma:
giant cell glioblastoma, gliosarcoma, epithelioid glioblastoma [14, 15, 18].

1.4.2 Molecular Pathology

Molecular studies on glioblastomas have enabled higher diagnostic accuracy and standardization, as well as provided markers to assess oncological prognosis and the predictive value of both conventional and targeted therapies.

1.4.2.1 IDH

IDH1 and IDH2, localized to the cytoplasm and mitochondria respectively, use nicotinamide adenine dinucleotide phosphate (NADP +) as a cofactor to catalyze the conversion of isocitrate to α-ketoglutarate (α-KG). The missense cancer-associated mutations are heterozygous and typically occur at Arginine 132 in IDH1 and Arginine 172 in IDH2, impairing the ability of mutant IDH to bind isocitrate. Additionally, the mutation results in the acquisition of a new activity promoting the conversion of α-KG to D-2-hydroxyglutarate (D-2-HG), which accumulates at very high levels [19].
High levels of D-2-HG have a significant impact on the epigenetic program of tumor cells. Specifically, D-2-HG acts as a competitive inhibitor of ten-eleven translocation (TET) family of DNA hydrolases and histone demethylases, both of which play a crucial role in maintaining the epigenetic state of a cell. The epigenetic reprogramming, in turn, may lead to tumorigenesis through inappropriate silencing of tumor suppressor

genes or activation of oncogenes. Elevated D-2-HG has direct metabolic consequences as tumor cells compensate for depletion of α-KG from the citric acid cycle [19]. **(Fig. 8)**

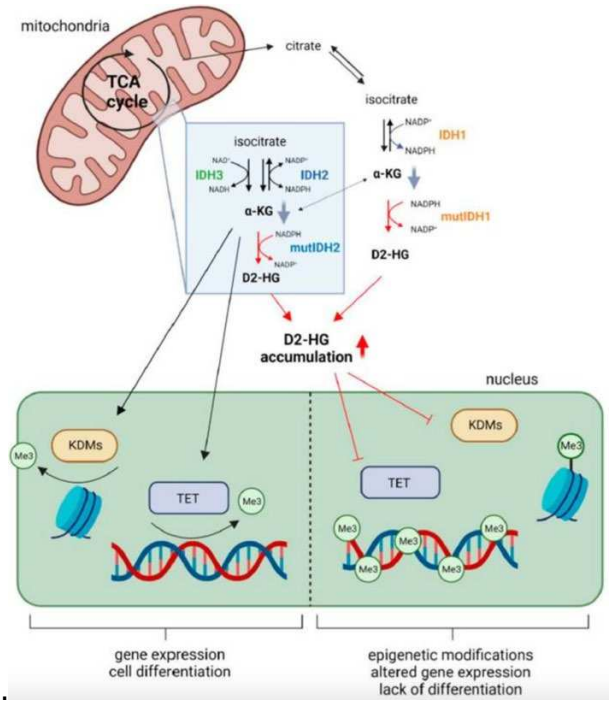

Fig. 8 The role of mutant or wild-type IDH and their downstream effects [20].

IDH1 and IDH2 mutations appear mutually exclusive, with some rare exceptions [20]. IDH1 is mutated in a vast majority of astrocytic and oligodendroglial neoplasms with WHO grade 2–3, as well as in secondary GBM (WHO grade 4). IDH1 mutation is very rare in primary GBM [14].

In the 2016 WHO classification, GBM was separated into IDH-wild-type and IDH mutant subtypes based on the mutation status of IDH1/2 genes [14]:

- Glioblastoma, IDH-wildtype (approximately 90% of cases): this subtype most commonly corresponds to glioblastoma clinically defined as primary or de novo. It predominates in patients over 55 years old [5].
- Glioblastoma, IDH-mutant (approximately 10% of cases): this subtype corresponds to glioblastoma clinically defined as secondary, originating from a pre-existing lower-grade diffuse glioma. It predominates in younger patients [5].

According to the latest WHO 2021 Classification, glioblastomas are defined as grade 4 lesions that are IDH-wildtype. High-grade lesions that are IDH-mutant are no longer classified as glioblastomas but rather as astrocytomas, IDH-mutant, grade 4. This classification shows significant difference in prognosis between these two tumor types, with IDH-wildtype glioblastomas typically having a poorer prognosis [6].
In fact, all patients with mutated IDH1 or IDH2 have shown greater survival compared to patients with IDH-wildtype, likely due to the sensitization of glioma cells to chemotherapy or radiotherapy generated by the reduction of intracellular NADPH pools [21-23].

1.4.2.2 TP53

The TP53 gene encodes the p53 protein, named the "Guardian of the Genome". p53 plays a central role in maintaining cellular homeostasis and is frequently deregulated in cancer. The protein is responsible of the control of cell proliferation, survival, genome integrity and other functions.

TP53 is one of the most commonly altered genes in cancer. The p53 pathway is also frequently deregulated in GBM. Alterations of tumor suppressor p53 are the most common, seen in 25–30 % of primary GBM and 60–70 % of secondary GBM. These alterations generally result in loss-of-function, gain-of-function, and dominant-negative mutational effects for p53, however, the distinct effect of these mutation types in GBM pathogenesis remains unclear [25].

The mutational status of TP53 is associated with GBM progression and p53 inactivation is correlated with a more invasive, less apoptotic, more proliferative, and more stem-like phenotype. Altered TP53 and its various pathway elements (ARF-MDM2/4) has not been correlated with survival in GBM, despite the high mutation frequency [24].

The most frequently deregulated component of the p53 pathway is a homozygous deletion of the CDKN2A/ARF locus, which occurs in ~60% of all GBM cases.
Most TP53 gene alterations in GBM are missense mutations in the DNA binding domain (DBD), leading to inhibition of transcription factor activity. Mut-p53 protein is highly

expressed in GBM and numerous studies have demonstrated that mut-p53 have oncogenic functions [24].

1.4.2.3 ATRX

ATRX (Alpha-Thalassemia mental Retardation X-linked) is a histone chaperone protein, member of the SWI/SNF superfamily of chromatin-remodeler proteins, that loads histones onto telomeres and maintains heterochromatin environments. ATRX also forms a complex with Death Domain-Associated Protein (DAXX) to deposit the histone variant H3.3 at nucleosomes [26].

ATRX is a major component of many critical cellular pathways, and new evidence shows that it is also critical in DNA replication and repair, advanced chromatin regulation, and gene transcription regulation [28].

ATRX-deficient tumors maintain telomere length in a telomerase-independent manner, called alternative lengthening of telomeres (ALT). The ATRX protein has been shown to inhibit ALT, and when mutated, the affected tumor cells are able to maintain telomere extension through homologous recombination (HR) [26].

ATRX mutations occur in approximately 57% of secondary glioblastomas, but they are rare in primary glioblastomas. In grade 4 gliomas, ATRX mutations are often accompanied by IDH1 and TP53 mutations [27]. ATRX is also a prognostic factor in gliomas. Among tumors with IDH mutations and no loss of chromosome 1p/19q, loss of ATRX is associated with improved progression-free and overall survival ATRX mutations are a good prognostic factor [29].

1.4.2.4 MGMT

O6-methylguanine-DNA methyltransferase (MGMT) is a DNA "suicide" repair enzyme. It repairs damaged guanine nucleotides by transferring the methyl at O6 site of guanine to its cysteine residues, thus avoiding gene mutation, cell death and tumorigenesis caused by alkylating agents [30]. The expression of MGMT gene is mainly regulated by epigenetic modification. Many studies have shown that the loss of MGMT expression is not due to gene deletion, mutation, rearrangement or unstable RNA, but due to methylation of CpG island of MGMT promoter [30].

If correctly transcribed, MGMT catalyzes the removal of methyl adducts at the O6 position of guanine caused by alkylating agents at the DNA level, transferring the methyl group from O6-methylguanine to the MGMT protein itself, thereby maintaining genomic stability and defending the cell against mutational insults [31] **(Fig. 9)**

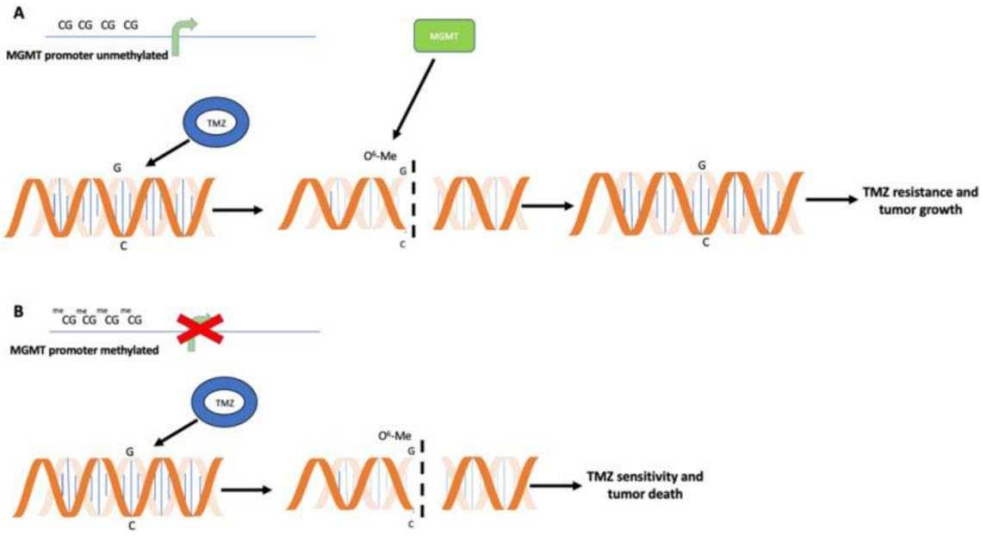

Fig. 9 DNA repair mechanism by MGMT in the tumor cell.
A) Unmethylated MGMT; B) Methylated MGMT [31].

However, this DNA repair mechanism takes on a completely opposite significance when maintained by the tumor cell: in fact, the correct function of the methyltransferase makes neoplastic cells resistant to alkylating drugs used in chemotherapy, like the commonly used temozolomide [32].

The MGMT promoter is methylated in 50% of glioblastomas and has emerged as one of the main prognostic factor and a predictor of response to temozolomide in patients with primary glioblastoma. However, several studies have shown that it is also prognostic for recurrent glioblastoma, with a survival increase of about 3-4 months [33].

1.4.2.5 TERT

The telomerase reverse transcriptase (TERT) gene encodes a highly specialized reverse transcriptase, which adds hexamer repeats to the 3′ end of chromosomes [14]. Telomeres are chromosome termini that contain repetitive DNA sequences (TTAGGG) [34] and are required for chromosomal integrity. Telomeres shorten at every cell cycle,

eventually leading to cell death or senescence. Telomerase is responsible for the repair of telomeres in order to maintain their length and avoid cell death. Telomere lengthening is required to achieve the infinite proliferation of cancer cells; thus, telomerase activity has been investigated as a potential mechanism for cancer growth [35].

Telomeres, without the presence of telomerase function, become progressively shorter at each cell division. Loss of telomere length beyond a certain point may cause chromosomal instability and genomic rearrangement. Thus, telomere shortening has important implications for cell proliferation [34].

Alterations in TERT promoter have been reported in up to 80% of glioblastomas [35]. Two mutually exclusive mutations in the human TERT promoter (pTERT) region, C228T and C250T, are important as they promote the formation of a novel binding site for transcriptional enhancers [34]. **(Fig. 10)**

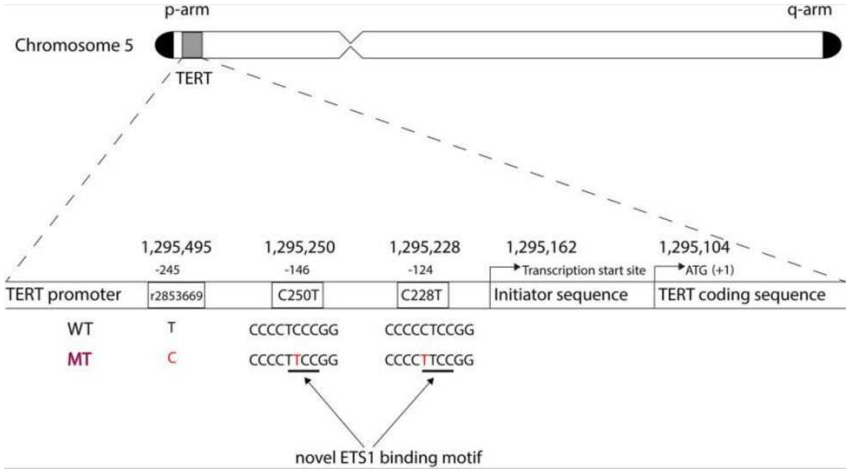

Fig. 10 TERT promoter mutations C250T and C228T. -146 and -124 indicate the position of the C250T and C228T mutations upstream, respectively, in relation to the start of the TERT coding sequence ATG [34].

They are more common in IDH1-wild type GBMs but rare in secondary (IDH1 mutant) GBMs and other astrocytomas. TERTp-mutation is associated with poor outcomes in patients with GBM. Several studies indicate that about 75% GBMs were associated with TERTp-mutation, TERTp-mut was associated with IDH-wt, EGFR amplification, CDKN2A deletion, and chromosome 10q loss, but not with MGMT promoter methylation. TERTp-mutation was an independent factor for poor prognosis [14].

1.4.2.6 EGFR

Epidermal Growth Factor Receptor (EGFR) is a transmembrane tyrosine kinase receptor that plays a significant role in the regulation of mitosis, differentiation, cell survival, and apoptosis.

The tyrosine kinase domain of EGFR is frequently altered in IDH-wildtype GBM. Overall, about 60% of tumors show evidence of EGFR amplification, mutation, rearrangement, or altered splicing. The most frequent EGFR alteration is amplification., which occurs in about 40% of IDH-wild type GBMs. In the majority of cases, EGFR amplification is associated with a second EGFR alteration, such as extracellular domain mutations or in-frame intragenic deletions encoding either EGFRvIII or other alternative transcripts [14].

EGFR amplifications have been reported to indicate a much more aggressive tumor subpopulation but several studies suggest that the influence of EGFR status on prognosis could be more complicated. Patients with EGFR amplifications had a better prognosis in the TERT-mutated context than patients with TERT-wildtype tumors. On the other hand, EGFR-wildtype GBM patients had longer survival with TERT-wildtype than patients with EGFR-wildtype and TERT-mutated. Therefore, further research is required to determine their multi-genic interaction [36].

Moreover, specific mutations can have a positive predictive value, as they are currently the subject of research and study for targeted monoclonal antibodies [36].

1.4.2.7 Other relevant molecular biomarkers in Glioblastoma

CDKN2A

Cyclin-dependent kinase inhibitor 2A (CDKN2A) is located on the short arm of chromosome 9 and encodes two tumor-suppressor proteins that regulate the activities of p53 and pRB in tumor suppression [37]. In several tumor subtypes, homozygous deletion of CDKN2A is associated with increased carcinogenesis and a poor prognosis [36]. Moreover, some studies have reported the CDKN2A/B homozygous deletion to be associated with unfavorable outcomes for all IDH-mutant astrocytoma grades (WHO grades II–IV) and IDH-wildtype GBM [38].

BRAF

B-Raf (encoded by the BRAF gene) is a serine/threonine-protein kinase, member of the RAS/RAF/MEK/ MAPK that functions downstream of EGFR. The canonical BRAF p.V600E mutation occurs in roughly half of all epithelioid GBM, but it is rare in classic GBM, detectable in only 1-2% of cases [39-40]. BRAF V600E and canonical IDH gene mutations are mutually exclusive. There are still little data investigating the prognostic role of BRAF V600E mutation in GBM [40].

PTEN

Phosphatase and tensin homolog (PTEN) is a tumor suppressor gene, playing important roles in the regulation of cell proliferation, adhesion and invasion, apoptosis, and DNA damage repair [41]. It antagonizes oncogenic PI3-kinase signaling. Due to its critical role in suppressing the potent signaling pathway, it is one of the most mutated tumor suppressors, especially in brain tumors. It is generally thought that PTEN deficiencies predominantly result from either loss of expression or enzymatic activity [42]. Mutations at the PTEN gene are found in 15–40% of primary GBMs but are absent in IDH1 mutated secondary GBMs and other lower-grade gliomas [14]. Importantly, PTEN deficiency in GBM has been associated with poor survival [42].

FGFR

Fibroblast Growth Factor Receptors (FGFR) form a family of four highly conserved transmembrane tyrosine kinase receptors (FGFR1-4) and a receptor that can bind the same ligands but lacks an intracellular kinase domain (FGFR5) [43]. FGFRs control many biological functions, including cell proliferation, survival, and cytoskeletal regulation. FGFR expression changes in astrocytes can lead to malignant transformation and GBM progression due to the activation of mitogenic, migratory, and antiapoptotic responses [43].

Gene expression analysis revealed high heterogeneity of FGFR1–4 expression in glioblastoma patients. Several studies have reported that FGFR1 and FGFR2 gene amplification, abnormal activation, or single nucleotide polymorphisms (SNPs) have a key role in glioblastoma progression. Moreover, a recent report found that FGFR3 and FGFR4 are also expressed in invasive glioblastoma cells. Scientific evidence reveals that

human glioblastoma is also characterized by oncogenic fusions involving the tyrosin kinase domain of FGFR3 and FGFR1 and to the transforming acidic coiled-coil (TACC) proteins [44].

1.4.3 Treatment

Despite significant progress in glioblastoma therapy, including a multimodal approach of surgery, radiotherapy, systemic therapy, and supportive care, the overall prognosis remains poor, and long-term survival is rare. Treatment strategies for glioblastoma are tailored based on each patient's characteristics, including age, performance status, radiological images, disease progression rate, and clinical, histopathological, and molecular diagnosis [45].

The current algorithm for treating IDH-wildtype glioblastomas, as defined by the latest WHO 2021 classification, is shown in **Fig. 11**. Younger patients and/or those with a good performance status, regardless of MGMT gene methylation status, generally have more treatment options post-surgery, which include radiotherapy, temozolomide, TTF (Tumor Treating Fields), and access to clinical trials. This differs for patients aged 70 and older or those of any age with poor performance status [8].

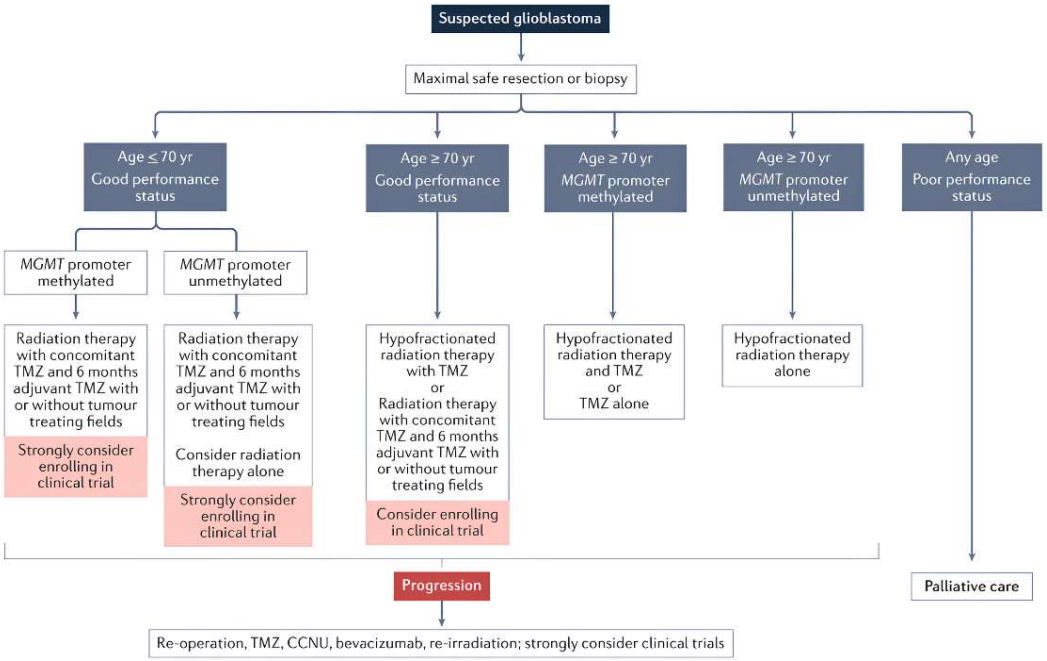

Fig. 11 The current algorithm for treating IDH-wildtype grade 4 glioblastomas, as defined by the latest WHO 2021 classification [8].

The current standard of care for newly diagnosed glioblastoma patients, known as the "Stupp protocol," includes:

- Surgical resection
- Radiotherapy and concomitant chemotherapy with temozolomide
- Adjuvant chemotherapy with temozolomide [46]

2. OBJECTIVE OF THE THESYS

The main goal of the study was to molecularly characterize a cohort of 19 patients retrospectively selected with a diagnosis of IDH-wildtype glioblastoma and a survival equal to or greater than 25 months. Through integrated analysis of molecular biomarkers including IDH, MGMT, TERT, H3F3A, HIST1H3B, determination of microsatellite instability, evaluation of immunohistochemical expression of p53 and ATRX, and exploration of a gene panel using Next-Generation Sequencing (NGS), we tried to identify specific genetic and molecular alterations that may be correlated with the favorable prognosis observed in this subset of patients.

3. MATERIALS AND METHODS

3.1 Materials

3.1.1 Instruments

- Rotary microtome (Leica Biosystems)
- DNA Extractor: MaxWell RSC (Promega)
- Thermoblock: ThermoMixer (Eppendorf)
- Thermocycler: Mastercycler nexus GX2 (Eppendorf)
- Sequencer: Genetic Analyzers 3130 (Applied Biosystems by Thermo Fisher)
- Fluorometer: Qubit™ 4 Fluorometer (Thermo Fisher Scientific)
- NGS platform: Genexus (Thermo Fisher Scientific)
- Immunostainer: BenchMark ULTRA (Ventana, Roche)
- Realtime PCR: EasyPGX qPCR instrument 96 (Diatech Pharmacogenetics)

3.1.2 Kit

- Maxwell RSC DNA FFPE Kit (Promega)
- Nuclease-Free Water, for Molecular Biology (Thermo Fisher Scientific)
- Qubit™ dsDNA Quantification Assay Kits ((Thermo Fisher Scientific)
- EpiJect Bisulfite Kit (Thermo Fisher Scientific)
- GeneScan, 500 LIZ, dye Size Standard (Applied Biosystems by Thermo Fisher)
- AmpliTaq Gold DNA Polymerase with Buffer II & MgCl2 (Applied Biosystems by Thermo Fisher)
- ExoProStar (Illustra)
- BigDye Terminator v1.1 Cycle Sequencing Kit (Applied Biosystems by Thermo Fisher)
- iX-Pure Dye Terminator Cleanup Kit (Resnova)
- Oncomine Precision Assay (Thermo Fisher Scientific)
- UltraView Universal DAB Detection Kit (Ventana, Roche)
- EasyPGX ready MSI (Diatech Pharmacogenetics)

3.1.3 Software

- Armonia
- BB Traccia
- OK-DH
- SPSS Statistics

3.2 Methods

3.2.1 Patients selection criteria

The study was conducted on a cohort of patients diagnosed with glioblastoma (WHO 2021 or earlier) between 2013 and 2022, retrospectively selected from the SCDU Pathological Anatomy database of "AOU Maggiore della Carità" in Novara. The patients in the study underwent surgery at the Neurosurgery Unit of "AOU Maggiore della Carità" in Novara. The study protocol was approved by the Ethics Committee of the "AOU Maggiore della Carità" in Novara and was conducted in accordance with the current revision of Helsinki Declaration.

Three software tools were used for case selection:

- Armonia, for searching patients and their histological and molecular reports.
- BB Traccia, for requesting of sample inclusions from the archive where they are stored.
- OK-DH, for finding information related to the post-surgical oncological follow-up.

The following information was collected:

- Complete demographic data;
- Date of diagnosis and histological report;
- IDH1 and IDH2 status, MGMT status, and other molecular investigations;
- Age at diagnosis;
- Age at death.

Patients with the following criteria were included in the study:

- Diagnosis of glioblastoma, IDH-wildtype;

- Survival ≥ 25 months.

Eligible patients, with a diagnosis of glioblastoma, IDH-wildtype, and survival of 25 months or more, were further characterized by collecting information on:

- Location and laterality of the lesion;
- Clinical history, signs, and symptoms at presentation;
- Date and type of surgical intervention;
- Radicality of the surgical intervention;
- Post-surgical therapeutic process;
- Disease recurrence.

Only patients meeting the following criteria were included:

- Macroscopically radical surgical intervention;
- History of active disease treatment at the SCDU Oncology and Radiotherapy unit of "AOU Maggiore della Carità" in Novara.

Information related to the surgical intervention and therapeutic process was obtained from the examination of reports of surgeries performed at the Neurosurgery Unit of "AOU Maggiore della Carità" in Novara and from the reports of oncological and radiotherapy visits conducted at the SCDU Oncology and Radiotherapy of "AOU Maggiore della Carità" in Novara.

To obtain follow-up information for that patients who had surgery at "AOU Maggiore della Carità" in Novara, but continued their therapeutic process in other structures, it was necessary to request information from the radiotherapy department of "Giuseppe Castelli" Hospital in Verbania-Pallanza.

3.2.2 Preparation of samples

The surgical specimens from the patients involved in the study were fixed in neutral buffered formalin for about 24 hours, then reduced and processed according to routine histopathological procedures, and finally embedded in paraffin. Sections cut from the paraffin blocks were stained with hematoxylin and eosin. The correct staging described

in histological report was verified by a pathologist, and a representative area of the lesion with a sufficient number of neoplastic cells was selected on the hematoxylin-eosin stained section. After performing a macrodissection with a scalpel on the block to circumscribe the area of interest, some sections, cut using a microtome, were put in a tube in order to proceed with the DNA extraction. In addition, two sections, each 3 μm thick, were placed on slides to undergo immunohistochemical reactions.

3.2.3 DNA extraction

After cutting 5 FFPE tissue sections, each 5 μm thick, and placing them in 1.5 ml tubes, DNA extraction was carried out using a magnetic bead extraction method with the Maxwell® RSC DNA FFPE kit from Promega. The complete procedure is showed below:

1. add 300 μl of Mineral Oil to each sample tube and vortex for 10 seconds;
2. heat the sample at 80°C for 2 minutes, then place sample at RT;
3. prepare a master mix composed by 224 μl of Lysis Buffer, 24 μl of Proteinase K Solution and 1 μl of Blue Dye for each sample;
4. add 250 μl of master mix to each sample tube and vortex for 5 seconds;
5. centrifuge sample tube at 10,000 x g for 20 seconds to separate layers;
6. transfer the sample tube to a 56°C heat block and incubate for 30 minutes;
7. transfer the sample tube to a 80°C heat block and incubate for 4 hours;
8. remove the sample tube from the heat block and allow the sample to cool to RT for 5 minutes;
9. centrifuge the sample tube at full speed in a microcentrifuge for 5 minutes;
10. immediately transfer the blue, aqueous phase containing the DNA to well #1 of a Maxwell® FFPE Cartridge, previously inserted in the deck-tray of the instrument;
11. place the RSC tip in well #8 of the same MaxWell FFPE Cartridges and insert of a 0.5 ml elution Eppendorf tube with 55 μl of Nuclease-Free Water onto the deck tray;
12. Transfer the deck tray into the MaxWell RSC automatic extractor (Promega), programming it, and starting the run.

At the end of the extraction, the extracted DNA was quantified using the Qubit™ 4 Fluorometer (Thermo Fisher Scientific) with the Qubit™ dsDNA HS Assay Kit, as described below **(Fig. 12)**:

1. set up 2 assay tubes for the standards and 1 assay tube for each sample;
2. prepare the Qubit™ working solution by diluting the Qubit™ reagent 1:200 in Qubit™ buffer. Calculate 200 µl of working solution for each standard and sample;
3. vortex all tubes for 2-3 seconds;
4. incubate the tubes for 2 minutes at RT;
5. insert the tubes in the Qubit™ Fluorometer and take readings.

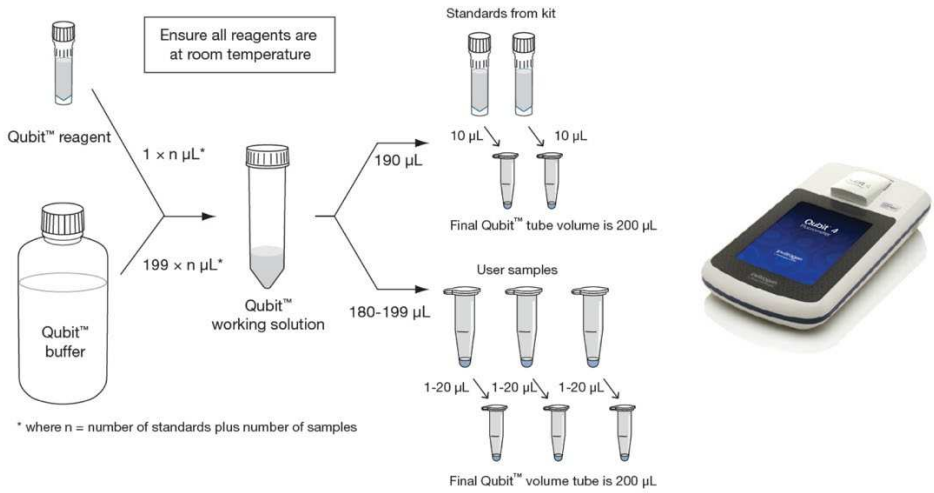

Fig. 12 Overview of the Qubit™ dsDNA HS assay used with a Qubit™ 4 Fluorometer.

3.2.4 Epigenetic evaluation of the MGMT gene

After DNA extraction and quantification, sample's DNA was diluted with Nuclease-Free Water to obtain a DNA amount between 200 and 500 ng in a final volume of 20 µl.
To evaluate the methylation status of the MGMT gene, the EpiJect Bisulfite Kit (Thermo Fisher Scientific) was used: 120 µl of modification reagent, containing sodium bisulfite, were added to 20 µl of DNA sample in order to selectively convert unmethylated cytosines into uracil.
After the purification of the converted DNA, two separate PCRs were performed using specific primers for the methylated allele (sequence containing methylated cytosines)

and the unmethylated allele (sequence containing unmethylated cytosines). The specific primers are described in **Table 1**.

GENE	PRIMER	PRIMER SEQUENCE
methylated MGMT	MET forward	6FAM-TTTCGACGTTCGTAGGTTTTCGC
	MET reverse	GCACTCTTCCGAAAACGAAACG
unmethylated MGMT	UNMET forward	T6FAM-TTTCGACGTTCGTAGGTTTTCGC
	UNMET reverse	AACTCCACACTCTTCCAAAAACAAAACA

Tab. 1 Sequence primers for the analysis of the MGMT gene.

The thermal protocols for the two PCRs are described in **Table 2**.

TIME	TEMPERATURE	CYCLES
5 minutes	95°C	1
30 seconds	92°C	5
2 minutes	51°C (M) 50°C (U)	
3 minutes	72°C	
30 seconds	95°C	35
1 minute	56°C (M) 55°C (U)	
3 minutes	72°C	
60 minutes	60°C	1

Tab. 2 Thermal protocol for the amplification reactions of MGMT genes.
(M) annealing temperature for methylated primers, (U) annealing temperature for unmethylated primers.

The PCR product was loaded onto the automatic sequencer Genetic Analyzer 3130 (Applied Biosystems by Thermo Fisher), diluted in a mix of formamide and fluorescent molecular weight marker (GeneScan, 500 LIZ, dye Size Standard - Applied Biosystems by Thermo Fisher). The instrument performs capillary electrophoresis, allowing visualization of the PCR products through fragment analysis. This results in two peaks, one corresponding to the methylated component and the other to the unmethylated component, measuring 81 bp and 91 bp respectively **(Fig. 13)**.

If both components are present in the analyzed sample, the ratio (R) between the methylated and unmethylated values is calculated. If $R \geq 0.1$, the sample was considered as methylated.

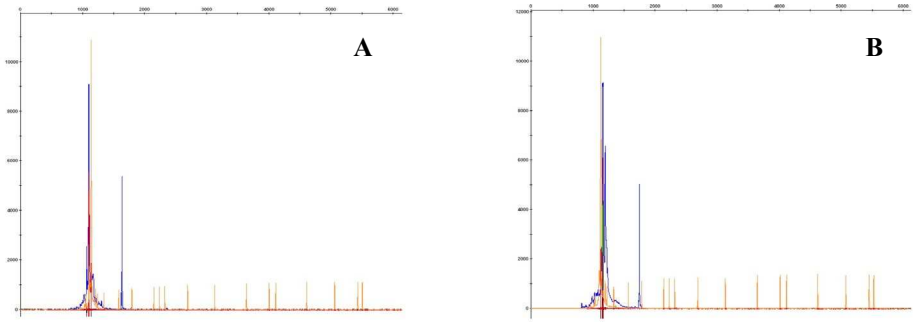

Fig. 13 Capillary electrophoresis of the PCR product (blue fragment) using the automatic sequencer. The molecular weight marker is shown in orange. A) Methylated MGMT; B) Unmethylated MGMT.

3.2.4 Sanger sequencing

For the detection of mutations in the IDH1, IDH2, pTERT, H3F3A, and HIST1H3B genes, Sanger sequencing was employed. First, the gene sequences of interest were amplified using Polymerase Chain Reaction (PCR) using a master mix prepared as showed in **Table 3**.

A) REAGENT	CONC	VOL	B) REAGENT	CONC	VOL
AmpliTaq Gold 360 MasterMix		10 µL	AmpliTaq Gold 360 MasterMix		10 µL
Primer forward	10 pM/µL	1 µL	Primer forward	10 pM/µL	1 µL
Primer reverse	10 pM/µL	1 µL	Primer reverse	10 pM/µL	1 µL
Nuclease free-water		3 µL	Nuclease free-water		1 µL
DNA template	20 ng/ µl	5 µL	10% 360 GC Enhancer		2 µL
			DNA template	20 ng/ µl	5 µL
FINAL VOLUME		20 µl	**FINAL VOLUME**		20 µL

Tab. 3 A) List of reagents and their respective volumes used for the amplification of the IDH1, IDH2, H3F3A, and HIST1H3B genes. B) The amplification of the TERT promoter involves the addition of 360 GC Enhancer to increase the specificity of the reaction due to the high GC content of this region.

Each sample was amplified separately using specific primer pairs for each gene. The specific primers are described in **Table 4**.

GENE	PRIMER	PRIMER SEQUENCE
IDH1	IDH1 forward	CTCCTGATGAGAAGAGGGTTG
	IDH1 reverse	TGGAAATTTCTGGGCCATG
IDH2	IDH2 forward	TGGAACTATCCGGAACATCC
	IDH2 reverse	AGTCTGTGGCCTTGTACTGC
hTERT	hTERT forward	TCCTGCCCCTTCACCTT
	hTERT reverse	AGCACCTCGCGGTAGTGG
H3F3A	H3F3A forward	GTGATCGTGGCAGGAAAAGT
	H3F3A reverse	CAAGAGAGACTTTGTCCCATTTT
HIST1H3B	HIST1H3B forward	GTTTTGCCATGGCTCGTACT
	HIST1H3B reverse	AAGCGAAGATCGGTCTTGAA

Tab. 4 List of sequence primers for the analysis of IDH1, IDH2, TERT promoter, H3F3A, and HIST1H3B genes.

For samples with a low concentration of genomic DNA, to ensure the success of the reaction, the volume of DNA template was increased, consequently reducing the volume of nuclease-free water, thus ensuring a final DNA concentration of at least 1 ng/µl.

For all PCR reactions, the thermal protocol was the same, as described in **Table 5**.

TIME	TEMPERATURE	CYCLES
10 minutes	95°C	1
15 seconds	95°C	45
30 seconds	52°C	
30 seconds	72°C	
3 minutes	72°C	1

Tab. 5 Thermal protocol for the amplification reactions of the IDH1, IDH2, TERT promoter, H3F3A, and HIST1H3B genes.

The amplified DNA was purified using ExoProStar reagent (Illustra). 2 µl of reagent were added for every 5 µl of amplified product, followed by incubation at 37°C for 15 minutes and then at 80°C for 15 minutes. The purified fragments were subjected to a

sequencing PCR using the BigDye Terminator v1.1 Cycle Sequencing Kit (Applied Biosystems by Thermo Fisher) and specific primers for each gene, as summarized in **Table 6**.

REAGENT	CONC	VOL
BigDye Terminator v1.1 Cycle Sequencing		1 µl
Primer	3,2 pM/µl	1 µl
Nuclease free-water		6 µl
Purified DNA		2 µl
FINAL VOLUME		10 µl

Tab. 6 List of reagents used for the sequencing reaction.
Forward primers were used for IDH1, IDH2, H3F3A and HIST1H3B genes,
and reverse primer for the TERT promoter gene.

The reaction occurred using the following thermal profile: 96°C for 10 seconds, 50°C for 5 seconds, and 60°C for 4 minutes repeated for 25 cycles.

After the sequencing reaction, a second purification step was performed: 49.5 µl of iX-Pure Resin and 11 µl of iX-Pure Activator were added to the PCR product. The purified sequences were incubated in a shaking thermoblock at 2000 rpm at RT for 30 minutes. Subsequentially, to each well of a 96-well plate containing 10 µl of formamide, 10 µl of purified sequences were added. The plate, previously denatured at 96°C for 3 minutes, was loaded onto a Genetic Analyzer 3130 automatic sequencer with 4 capillaries (Applied Biosystems by Thermo Fisher).

The resulting electropherograms were analyzed by comparing the obtained sequences with reference sequences to identify the presence of hotspot mutations in reference codons.

3.2.5 Next Generation Sequencing (NGS)

In order to evaluate different genes associated with the genomic landscape of glioblastoma, the multigene panel Oncomine Precision Assay (ThermoFisher Scientific), validated for the platform NGS Genexus Integrated Sequencer (ThermoFisher Scientific), was used.

This system performs a massive parallel sequencing, by integrating library preparation, templating, and sequencing into a single-day/single-instrument automated run.

After the DNA extraction, sample's DNA was diluted with Nuclease-Free Water to obtain a DNA concentration of 1 ng/µl in a final volume of 20 µl. Then 20 µl of diluted DNA of each sample were added into a 96-well plate and, after loading the pre-filled reagents and the plate onto the instrument, then the run was started.

The workflow of NGS run is showed in **Fig. 14**.

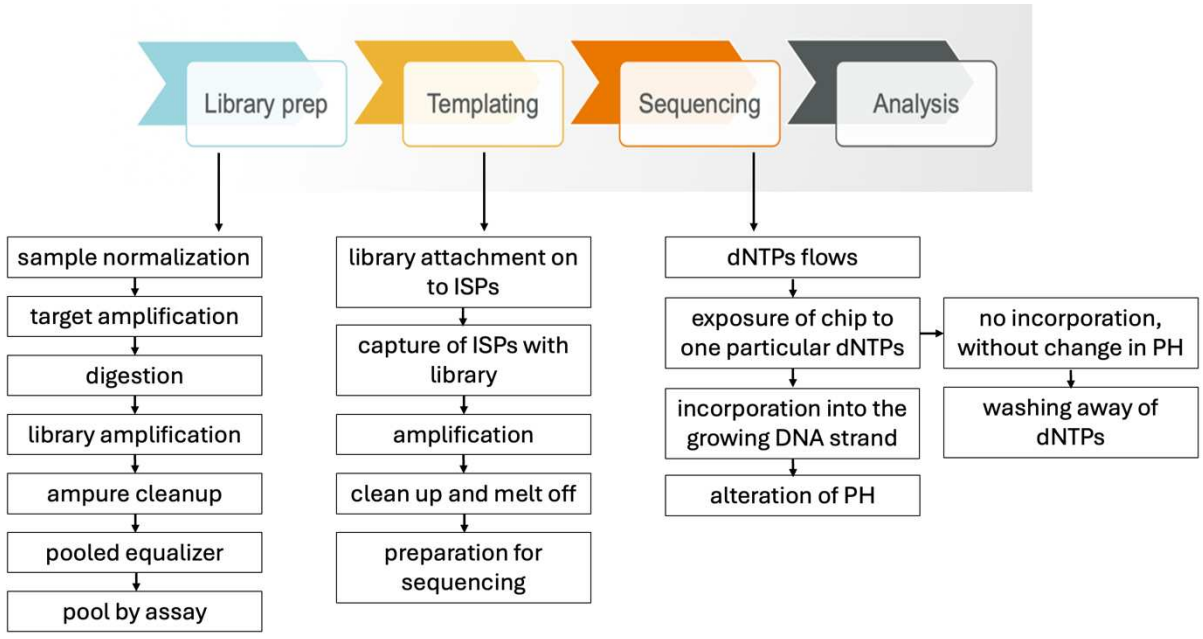

Fig. 14 The NGS workflow.

The multigene panel used, allowed for the simultaneous evaluation of hotspot mutations and copy number variation (CNV), by permitting to detect and annotate low frequency (to 0.5% limit of detection) somatic variants of the following genes:

DNA HOTSPOTS			CNV
AKT1	ESR1	MAP2K2	ALK
AKT2	FGFR1	MET	AR
AKT3	FGFR2	MTOR	CD274
ALK	FGFR3	NRAS	CDKN2A
AR	FGFR4	NTRK1	EGFR
ARAF	FLT3	NTRK2	ERBB2
BRAF	GNA11	NTRK3	ERBB3
CDK4	GNAQ	PDGFRA	FGFR1
CDKN2A	GNAS	PIK3CA	FGFR2
CHEK2	HRAS	PTEN	FGFR3
CTNNB1	IDH1	RAF1	KRAS
EGFR	IDH2	RET	MET
ERBB2	KIT	ROS1	PIK3CA
ERBB3	KRAS	SMO	PTEN
ERBB4	MAP2K1	TP53	

After the run was completed, the analysis of results began with an evaluation of run-level sequencing metrics. Specifically, the range of final reads should be between 40 and 52 million for a full chip run, with a loading density of at least 80%. Additionally, the percentage of the polyclonal component should be between 25% and 40%.

Next, the sample metrics for each DNA sample were controlled. The acceptable ranges for each parameter are shown in **Fig. 15**. If a DNA sample passed the instrument's quality control (**Fig. 16**), it proceeded to the evaluation of potential variants identified by software analysis.

Sample Metrics	Typical Range
Mapped reads	1-1.5 million (3-plex)
MAPD	<0.5
MRL	~90 bp
Median Read Cov	~2,500x
Median Mol Cov	>250
Uniformity	>90%

Fig. 15 Typical range of DNA sample metrics.

Fig. 16 Instrument's QC of a DNA sample.

3.2.6 Immunohistochemistry

The evaluation of p53 and ATRX expression was performed using immunohistochemistry on 3 µm thick sections of FFPE tissue. The staining procedure was conducted using the BenchMark ULTRA immunostainer (Ventana, Roche) with the ultraView Universal DAB Detection Kit (Ventana). For each sample, 2 sections were prepared, each placed on a polarized glass slide and incubated at 60°C for 20 minutes to remove the paraffin. Subsequently, the slides were loaded onto the immunostainer for further processing. The protocols and the antibodies used are summarized in **Table 7** and in **Table 8**, respectively.

TP53	ATRX
Deparaffinization	Deparaffinization
Antigen retrieval with ULTRA Conditioner (CC1) at 95°C for 36 minutes	Antigen retrieval with ULTRA Conditioner (CC1) at 95°C for 92 minutes
Primary antibody incubation for 24 minutes	Primary antibody incubation for 60 minutes
	Signal amplification with Amplifier (mouse)
Counterstaining with hematoxylin for 12 minutes	Counterstaining with hematoxylin for 12 minutes
Post-counterstaining with Bluing reagent for 4 minutes	Post-counterstaining with Bluing reagent for 4 minutes

Tab. 7 Immunohistochemical staining protocols.

ANTIBODY	SPECIES	CONCENTRATION	COMPANY
CONFIRM anti-p53 (DO-7)	Mouse	0,5 µg/ml	Ventana Medical System Inc.
Anti-ATRX	Rabbit	0,2 mg/ml (dilution 1:400)	Sigma-Aldrich Inc.

Tab. 8 Antibodies used for immunohistochemical investigations.

After staining completion, the slides underwent microscopic analysis, which included the assessment of the reaction adequacy and the count of positive cells.

For p53 and ATRX expression, a cutoff of 10% positive cells was considered. An expression of p53 above 10% may indicate a mutation in the TP53 gene, leading to altered physiological processes in protein degradation. Conversely, an expression of

ATRX below 10% may indicate a mutation in the ATRX gene, resulting in the absence of protein expression.

3.2.7 Determination of microsatellite instability

For the determination of microsatellite instability, the EasyPGX ready MSI kit (Diatech Pharmacogenetics), validated for the EasyPGX qPCR instrument 96, was used.

First, an end-point PCR was performed to selectively amplify DNA regions containing the analyzed microsatellites. Subsequently, a denaturation and hybridization step with marker-specific probes labeled with a reporter dye was carried out with the target DNA. The determination of microsatellite stability/instability was conducted by comparing the denaturation curves of each individual marker with a stable positive control.
The list of analyzed markers is reported in **Table 9**.

MARKER	GENE	CHROMOSOME
BAT25	cKIT	4 (4q12)
BAT26	MSH2	2 (2p21-p16.3)
NR21	SLC7A8	14 (14q11.2)
NR22	STT3A	11 (11q24.2)
NR24	ZNF2	2 (2q11.1)
NR27	BIRC3	11 (11q22.2)
CAT25	CASP2	Co 7 (7q34)
MONO27	MAP4K3	2 (2p22.1)

Tab. 9 Markers analyzed for the determination of microsatellite instability status.

The kit consists of 8-well strips (0.2 ml each) for end-point PCR and 8-well strips (0.2 ml each) for hybridization. Each well in both strips is designated for the analysis of a single microsatellite region and is preloaded with reagents in a dry format.
For the end-point PCR, 25 µl of DNA were added to each preloaded well containing the reagents. The strip was then loaded into the instrument and the run was started. Upon completion, the biotinylated amplification products on agarose bead streptavidin-coated were immobilized by adding a prepared immobilization mixture. This was

followed by denaturation of the immobilized products and transfer into the wells of the hybridization strip. The hybridization strip was then loaded into the instrument and the run was initiated.

After hybridization, the DNA undergoes gradual heating, generating denaturation curves that represent changes in fluorescence emitted by the probes separating from the DNA, in function to the temperature. The denaturation curves of each marker are compared with the positive control. Specifically, differences in melting temperatures (ΔTm) indicate variations in the length or sequence of microsatellite repeats. The melting temperature is the temperature at which 50% of the DNA is single-stranded.
Analysis of the results was conducted using EasyPGX Analysis Software.
The ΔTm values considered as cutoffs, for defining the stability/instability status of microsatellites, are reported in **Table 10**.

MARKER	ΔTm	RESULT
BAT25	< -3	BAT25 instable
BAT26	< -3	BAT26 instable
NR21	< -3	NR21 instable
NR22	< -3.5	NR22 instable
NR24	< -3	NR24 instable
NR27	< -3	NR27 instable
CAT25	< -3	CAT25 instable
MONO27	< -3.5	MONO27 instable
BAT25	≥ -3	BAT25 stable or below the detection limit
BAT26	≥ -3	BAT26 stable or below the detection limit
NR21	≥ -3	NR21 stable or below the detection limit
NR22	≥ -3.5	NR22 stable or below the detection limit
NR24	≥ -3	NR24 stable or below the detection limit
NR27	≥ -3	NR27 stable or below the detection limit
CAT25	≥ -3	CAT25 stable or below the detection limit
MONO27	≥ -3.5	MONO27 stable or below the detection limit

Tab. 10 ΔTm values for each marker, defining the stability/instability status of microsatellites.

The samples were evaluated considering the number of unstable markers, as reported in **Table 11**.

N° OF INSTABLE MARKER	GLOBAL STATUS OF INSTABILITY
0	stable
1	low instability (MSI-L) or below the detection limit
≥ 2	high instability

Tab. 11 Overall instability status assigned in based on the number of unstable markers.

3.2.8 Overall Survival analysis

In order to evaluate the overall survival of patients with IDH-wildtype glioblastoma selected in the study and the impact of various factors on the survival of long-term survivors, survival curves were constructed using the Kaplan-Meier analysis method (with SPSS Statistics Software). The effect of factors related to the clinical characteristics of the patient and the molecular characteristics of the tumor on survival was investigated using the Log Rank test. The results were considered significant for $p<0.05$ (*p-value*).

4. RESULTS

4.1 Selection of patients

332 patients with diagnosis of glioblastoma (WHO 2021) were initially selected between 2013 and 2022 at the AOU Maggiore della Carità in Novara.

As first inclusion criterion, the presence of IDH-wildtype status was considered. Among them, 13 patients were excluded due to IDH-mutant status, inadequate data, or other diagnoses.

Survival in months was calculated from the date of surgery to the date of death or the date of the last follow-up visit report, for patients still alive.

Of the 319 patients with a diagnosis of IDH-wildtype glioblastoma, 24 patients showed a survival of 25 months or more, and 215 patients showed a survival of less than 25 months. This selection necessarily led to the exclusion of 80 patients who were not followed up post-surgery at the AOU Maggiore della Carità in Novara, for whom the date of death was unknown.

Informations regarding the surgical procedure and its radicality, as well as the history of active therapy, both chemotherapy and/or radiotherapy were collected. This led to the exclusion of 2 patients due to subtotal surgical resection and 3 patients due to the unavailability of the aforementioned information. At the end of the selection process, out of the 332 eligible patients, 19 were confirmed in the study.

The described selection process is schematically shown in **Figure 17**.

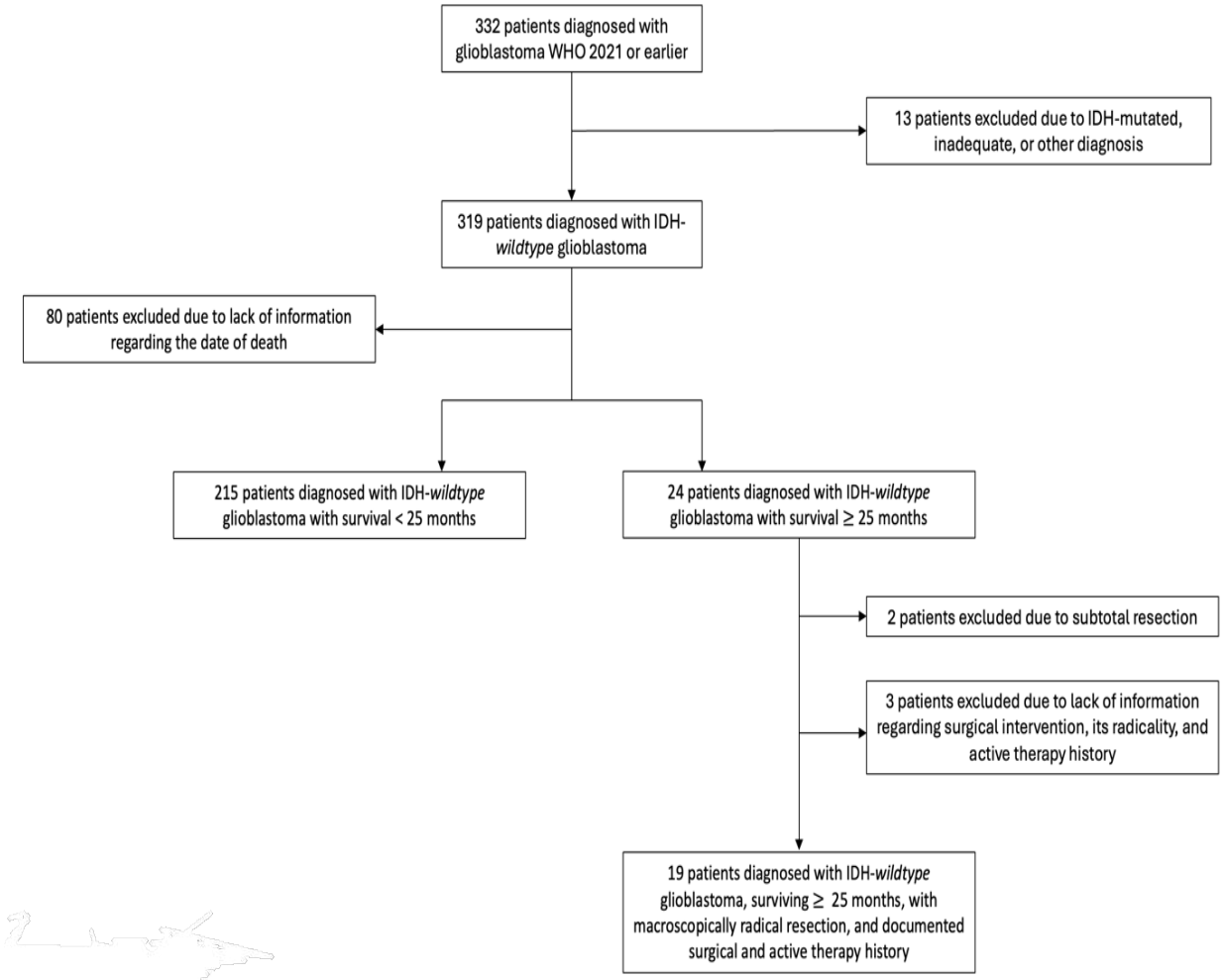

Fig. 17 Flow-chart representing the patient selection process.

4.2 Data analysis

The clinical-demographic and survival data of the 19 patients included in the study are summarized in **Table 12**.

PATIENTS	GENDER	AGE AT DIAGNOSIS	AGE AT DEATH	OS (days)	OS (months)
1	M	61	69	3024	99
2	F	46	48	845	27
3	F	43	45	1071	35
4	M	57	59	780	25
5	F	59	64	1710	56
6	M	68	70	872	28
7	F	15	22	2802	92
8	F	47	51	1188	39
9	M	59	62	1193	39
10	F	54	58	1324	43
11	M	43	46	1044	34
12	F	62	64	945	31
13	M	49	52	853	28
14	F	58	61	1070	35
15	M	68	70	764	25
16	F	52	alive	2004	65
17	M	71	alive	1907	62
18	M	73	76	1156	37
19	F	20	alive	1646	54

Tab. 12 Clinical-demographic and survival data related to: gender (M: male, F: female), age at diagnosis, age at death (if applicable), survival in days, survival in months (OS: Overall Survival). Patients still alive at the time of the study are shown in green.
The patient with the longest survival is highlighted in blue.

From data collected in **Table 13**, 9 patients (47%) are male and 10 (53%) are female. The average age at diagnosis is 53 years, with the youngest patient diagnosed at 15 years old and the oldest at 73 years old.

Of the 19 patients, 16 were deceased at the time of the study, and 3 were alive. Among the 16 deceased patients, the median age at death is 57 years old. The median Overall Survival (OS) is 45 months; the patient with the longest survival lived 99 months from diagnosis.

DATA		RESULTS	
		N	**%**
gender	male	9	47
	female	10	53
age at diagnosis	<40 yo	2	10
	40-59 yo	11	58
	60-75 yo	6	32
	average	53	
	median	57	
	range	15-73	
age at death	<40 yo	1	5
	40-59 yo	7	37
	60-75 yo	8	42
	alive	3	16
	average	57	
	median	60	
	range	22-76	
OS (days)	*average*	1379	
	median	1156	
	range	764-3024	
OS (months)	*average*	45	
	median	37	
	range	25-99	

Tab. 13 Clinical-demographic data divided by gender, age at diagnosis, age at death (if applicable), and survival data (OS: Overall Survival).

The methylation status of MGMT promoter was investigated at the time of diagnosis and results are reported in **Table 14**. Of the 19 patients in the study, 11 (58%) had methylated MGMT and 8 (42%) had unmethylated MGMT.

DATA		RESULTS	
		N	**%**
MGMT status	methylated	11	58
	unmethylated	8	42

Tab. 14 Data on the methylation status of MGMT.

All patients included in the study underwent a neurosurgical procedure and obtained

a macroscopically radical excision of the lesion.

Regarding the therapeutic approach (**Tab. 15**), 84% of patients underwent a treatment consisting of an initial phase of concomitant alkylating chemotherapy (temozolomide) and intensity-modulated radiation therapy (IMRT), followed by an adjuvant phase of chemotherapy with temozolomide (Stupp regimen). Two of these patients underwent additional treatment with a monoclonal antibody: one was treated with the anti-VEGF monoclonal antibody bevacizumab and the other one with ABT-414 (an anti-EGFR-amplified monoclonal antibody) on a compassionate use basis. Two patients (11%) received only radiotherapy after surgery, followed by adjuvant temozolomide, while one patient (5%), after concomitant radiotherapy and chemotherapy, did not receive adjuvant temozolomide.

DATA		RESULTS	
		N	**%**
therapy	concomitant radiochemotherapy	1	5
	concomitant radiochemotherapy + adjuvant chemotherapy	16	84
	radiotherapy + adjiuvant chemotherapy	2	11

Tab. 15 Data related to the therapy administered after surgery on the primary tumor.

All patients in the study experienced a recurrence, identified during follow-up. As reported in **Table 16**, 6/19 patients (32%) underwent a second surgery, while 13 patients (68%) did not have an indication for surgical intervention. For the 6 patients who underwent surgery, the diagnosis of glioblastoma was confirmed through histological and molecular evaluation. Most patients (89%), regardless of surgical intervention, received chemotherapy and/or radiotherapy for the recurrence.

DATA		RESULTS	
		N	**%**
recurrence	surgical intervention	6	32
	no indication for surgical intervention	13	68
	radiotherapy and/or chemotherapy	17	89
	no therapy	2	11

Tab. 16 Data related to the treatment of recurrence.

For completeness, **Table 17** reports the clinical-demographic data, survival data, and MGMT methylation status for the 215 patients diagnosed with IDH-wildtype glioblastoma, with a survival less than 25 months.

DATA		RESULTS	
		N	**%**
gender	male	127	59
	female	88	41
age at diagnosis	<40 yo	5	2
	40-59 yo	54	25
	>60 yo	156	73
	average	65	
	median	67	
	range	26-85	
age at death	<40 yo	5	2
	40-59 yo	48	22
	>60 yo	158	74
	alive	4	2
	average	66	
	median	68	
	range	27-85	
OS (days)	*average*	234	
	median	197	
OS (months)	*average*	7	
	median	6	
MGMT status	methylated	97	45
	unmethylated	92	43
	inadequate	26	12

Tab. 17 Clinical-demographic data categorized by gender, age at diagnosis, and age at eventual death, survival data (OS: Overall Survival), and MGMT methylation status data.

Comparing the clinical-demographic data in **Table 13**, related to the 19 patients diagnosed with IDH-wildtype glioblastoma with a survival ≥ 25 months, with the clinical-demographic data in **Table 17**, related to the 215 patients diagnosed with IDH-wildtype glioblastoma with a survival < 25 months, it emerges that:

- The mean and median age at diagnosis are lower in patients with survival ≥ 25 months (53 years vs. 65 years and 57 years vs. 67 years).
- The percentage of patients with methylated MGMT status is higher in patients with survival ≥ 25 months (58% vs. 45%), although it should be noted that in 12% of patients with survival < 25 months, the MGMT methylation status was unknown.

4.3 Immunohistochemistry results

For the evaluation of TP53 expression by using immunohistochemical staining, an immunoreactivity threshold of 10% was considered. Samples characterized by a percentage of stained nuclei > 10% were considered immunopositive; immunopositivity is indicative of a possible gene mutation and consequent protein retention. (**Fig. 18**)

For the evaluation of ATRX expression, the same immunoreactivity threshold was considered. However, the presence of a percentage of labeled nuclei > 10%, corresponding to immunopositivity, is indicative of normal protein expression and the absence of gene mutation. (**Fig. 19**)

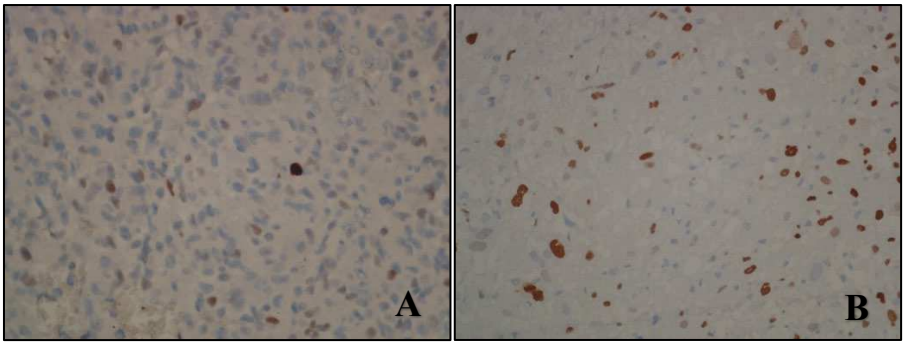

Fig. 18 Immunohistochemical staining for p53.
A) Immunonegative sample. B) Immunopositive sample.

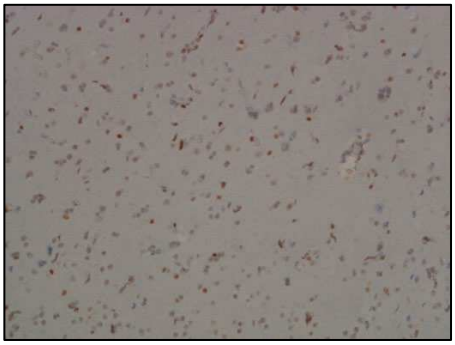

Fig. 19 Immunohistochemical staining for ATRX.: immunopositive sample.

The results of the immunohistochemical investigations for p53 and ATRX are reported in **Table 18**.

13/19 patients (68%) were found to be immunonegative for p53 and 5 (26%) results immunopositive. The sample from patient 14 showed no immunoreactivity for p53, indicating absence of protein expression.

Regarding ATRX, all samples expressed the protein, with a percentage of tumor cells labeled > 10%.

PATIENTS	TP53	ATRX	PATIENTS	TP53	ATRX
1	neg	pos	**11**	neg	pos
1R	neg	pos	**11R**	neg	pos
2	pos	pos	**12**	neg	pos
3	pos	pos	**13**	neg	pos
3R	pos	pos	**14**	0%	pos
4	neg	pos	**14R**	neg	pos
5	neg	pos	**15**	pos	pos
6	neg	pos	**16**	neg	pos
7	neg	pos	**17**	neg	pos
8	neg	pos	**18**	neg	pos
9	neg	pos	**19**	pos	pos
10	pos	pos	**19R**	pos	pos

Tab. 18 Results of immunohistochemical investigations for p53 and ATRX.
neg: immunonegative. pos: immunopositive. (R: recurrence).

4.4 Results of molecular investigations

The results of molecular investigations performed on the 19 samples of primary glioblastoma and the 5 recurrences, are reported in **Table 19**.

Out of 144 molecular investigations conducted via Sanger sequencing for the evaluation of pTERT, H3F3A, and HIST1H3B genes, 11 were deemed non-executable due to likely insufficient material or fragmented DNA.

PATIENTS	IDH1	IDH2	MGMT	pTERT	H3F3A	HIST1H3B	MSI
1	WT	WT	met	WT	WT	WT	MSS
1R	WT	WT	met	WT	WT	WT	MSS
2	WT	WT	unmet	**C228T**	WT	WT	MSS
3	WT	WT	unmet	WT	WT	WT	MSS
3R	WT	WT	unmet	WT	WT	WT	MSS
4	WT	WT	unmet	-	WT	WT	MSS
5	WT	WT	unmet	**C250T**	WT	WT	MSS
6	WT	WT	met	**C228T**	WT	WT	MSS
7	WT	WT	unmet	-	WT	-	MSS
8	WT	WT	met	-	-	WT	MSS
9	WT	WT	met	**C250T**	WT	WT	MSS
10	WT	WT	met	**C250T**	WT	WT	MSS
11	WT	WT	unmet	WT	WT	WT	MSS
11R	WT	WT	unmet	-	-	WT	MSS
12	WT	WT	met	**C250T**	WT	WT	MSS
13	WT	WT	unmet	**C250T**	WT	WT	MSS
14	WT	WT	met	WT	-	-	MSS
14R	WT	WT	met	**C250T**	WT	WT	MSS
15	WT	WT	met	WT	WT	WT	**MSI-L**
16	WT	WT	met	**C250T**	WT	WT	MSS
17	WT	WT	met	**C250T**	WT	WT	MSS
18	WT	WT	met	-	-	WT	MSS
19	WT	WT	unmet	WT	WT	WT	**MSI-L**
19R	WT	WT	unmet	WT	WT	WT	MSI-L

Tab. 19 Status of IDH1 and IDH2 and MGMT methylation, and results of molecular investigations on pTERT, H3F3A, and HIST1H3B, and evaluation of microsatellite instability. WT: WildType. MSS: Microsatellite Stability. MSI: Microsatellite Instability. MSI-L: Microsatellite Instability-Low. Met: methylated. Unmet: unmethylated.

From the data collected in **Table 20**, it emerges that:

- pTERT gene: of the 15 evaluable samples related to the primary tumor, 6 (40%) were non-mutated, 7 (47%) had the C250T mutation, and 2 (13%) had the C228T mutation.

- H3F3A and HIST1H3B genes: all evaluable samples related to the primary tumor were non-mutated.
- microsatellite instability: of the 19 primary tumors, 17 (89%) showed microsatellite stability (MSS), and 2 (11%) showed low microsatellite instability (MSI-L).

DATA		RESULTS	
		N	%
pTERT	WT	6	40
	C228T	2	13
	C250T	7	47
H3F3A	WT	16	100
	G34	0	0
	K27	0	0
HIST1H3B	WT	17	100
	K27	0	0
MSI	MSS	17	89
	MSI-L	2	11
	MSI-H	0	0

Tab. 20 Data on the results of molecular investigations on primary tumor samples.

Regarding recurrences **Table 19**:

- Patients 1, 3, and 19 maintained the same mutational profile as the primary tumor.
- Patient 11: it was not possible to evaluate pTERT and H3F3A, while HIST1H3B and MSI were confirmed as in the primary tumor.
- Patient 14 acquired a C250T mutation in the pTERT gene in the recurrence, which was not present in the primary tumor.

4.5 NGS results

Table 21 shows the results of the Next Generation Sequencing (NGS) analysis performed on 19 primary glioblastoma samples and 5 recurrences. It was not possible to evaluate the genetic panel for the sample from patient 7 due to insufficient material.

Therefore, sequencing results were obtained for 23 samples, 18 related to the primary tumor and 5 related to recurrences.

Hotspot mutations were found in BRAF, TP53, PTEN, EGFR, FGFR1, FGFR3, FGFR4, PDGFRA, CDKN2A, PI3KCA, GNA11, and NTRK3 genes, and Copy Number Variations were detected in EGFR, FGFR3, and CDKN2A genes.

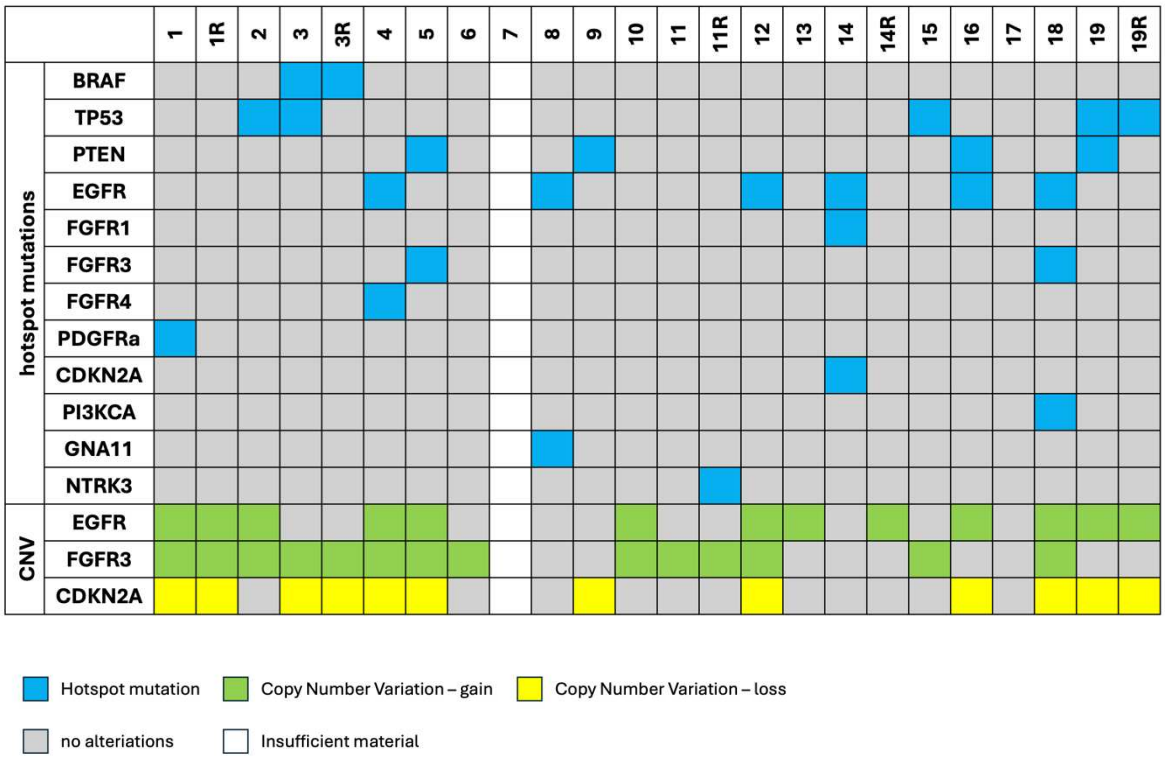

Tab. 21 Data on the results of the Next Generation Sequencing analysis.

As reported in **Table 22**, the most frequently mutated genes among the 18 analyzed samples from the primary tumor were: EGFR (33%), TP53 (22%), and PTEN (22%). Many samples showed amplification of EGFR and FGFR3, with 10 (55%) and 11 (61%) samples, respectively. Additionally, 9 samples (50%) exhibited deletion of CDKN2A.

DATA		RESULTS	
GENE	**VARIANT**	**N**	**%**
BRAF	p.V600E	1	5
TP53	p.R249S p.S240G p.Y220H p.R175H	1 1 1 1	22
PTEN	p.R130* p.R173C p.R130Q	2 1 1	22
EGFR	p.G598V p.A289D p.R108K p.A289V	1 2 1 2	33
FGFR1	p.R653*	1	5
FGFR3	p.K650E p.R248C	1 1	11
FGFR4	p.V550M	1	5
PDGFRa	p.H845Y	1	5
CDKN2A	p.A60V	1	5
PIK3CA	p.R88*	1	5
GNA11	p.E191K	1	5
EGFR	amplification	10	55
FGFR3	amplification	11	61
CDKN2A	deletion	9	50
≤ 3 genetic abnormalities		10	
> 3 genetic abnormalities		8	

Tab. 22 Data related to the NGS results on primary tumor samples.

4.6 Survival analysis

Within this thesis work, to study the possible prognostic value of gene alterations detected through molecular techniques, Kaplan-Meier survival curves were constructed. The values of the following variables, related to the 19 patients diagnosed

with IDH-wildtype glioblastoma and survival ≥ 25 months, were compared with overall survival:

- Amplification of FGFR3: FGFR3 amplified vs FGFR3 non amplified (p>0,05);
- MGMT status: methylated MGMT vs unmethylated MGMT (p>0,05);
- Mutational status of pTERT gene: pTERT WT vs pTERT mutant (p>0,05);
- Number of genetic abnormalities: >3 vs ≤3 (p>0,05);
- Amplification of EGFR: EGFR amplified vs EGFR non-amplified (p>0,05);
- Deletion of CDKN2A: CDKN2A deleted vs CDKN2A non-deleted (p>0,05).

The Kaplan-Meier curves constructed did not show statistically significant differences. Subsequently, the long-term survival patients were divided into two groups: with survival less than 40 months and more than 40 months. In this case, upon comparing the same variables by stratifying the patients into these two groups, it was found that only for FGFR3 amplification, the overall survival of patients without FGFR3 amplification was statistically superior (p<0,05) compared to patients with FGFR3 amplification in both groups, as shown in **Curve 1**.

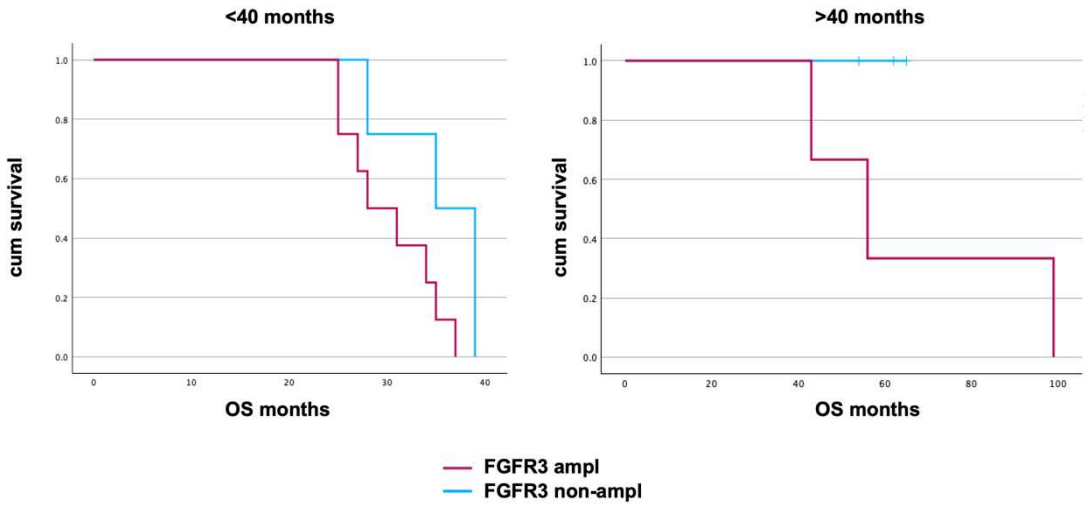

Curve 1 Survival curves comparing patients with FGFR3 amplified vs. non-amplified, stratified by patients with survival <40 months and >40 months. *P-value* = 0.0210.

5. DISCUSSION

Glioblastomas IDH-wild type, are characterized by a very poor prognosis with a median survival ranging from 8 and 12 months after diagnosis [47]. Standard therapeutical approaches include radical surgery, when possible, radiotherapy and chemotherapy with temozolomide in eligible patients [48]. However, although an improved survival has been obtained for this type of tumor after STUPP protocol, if we compare it with the survival in other types of tumors this improvement must be classified as poor [1]. Although factors that improve survival has been reported for glioblastoma, the percentage of patients with long term survival remains unchanged regardless the STUPP protocol and new therapeutical approaches based on targeting several genes, mutations, amplification or translocation.

Among several prognostic factors, the status of IDH 1 or 2 seem to be the most important one [49]; indeed, tumors with histological grade 4 and IDH 1-2 mutated have significantly better prognosis than the counterpart IDH wild type [50].

More recently authors have reported other positive prognostic factors [58-59], like younger age, histologic subtype (i.e. giant cell glioblastoma), microsatellite instability and MGMT promoter hypermethylation [51-54,57]. However, despite significant progress in identifying multiple molecular features, associated with aggressive behavior in subsets of histological low-grade astrocytomas, less progress has been made in identifying genetic feature associated with long survival in glioblastoma.

We selected 19 patients among 319 IDH-wild type glioblastomas, with more than 24 months of survival, all treated with radical surgery followed by radiochemotherapy, after histological revision by an experienced pathologist. All the cases were studied by immunohistochemistry searching for ATRX and P53 expression and by molecular methods including sanger sequencing for TERT, H3F3A, HIST13HB and next generation sequencing in order to search for mutations or amplification of the main gene involved in gliomagenesis.

Main recurrent mutations were EGFR, TP53, and PTEN, along with amplification of EGFR and FGFR3 and deletions of CDKN2A. Moreover, we identified also more sporadic mutations like BRAF, PDGFRA, PIK3CA and GNA11. In only 2 cases a low microsatellite instability was also identified.

Although none of these factors alone appear sufficient to confer better clinical outcome since this feature are also found in glioblastomas with significantly shorter survival times this work open the possibility to identify new therapeutical targets. For example, canonic mutation of BRAF may benefit of specific target therapy [55], as well as EGFR amplification [56] whereas microsatellite instability could be used for immunotherapy approach.

In this work we also divided long term survival patients in two groups: less than 40 months and more than 40 months. We found that patients without amplification of FGFR3 had a longer survival. This result should be considered as preliminary since the low number of patients included in the study, but could indicate that specific biomarker or biomarkers may justify an advantage of survival in a subset of glioblastoma patients. Obviously, more work is needed in order to explain the difference in terms of survival among glioblastoma patients that apparently are similar for histology and IDH status and full molecular characterization of large cohorts of patients focusing on those with long survival is needed to better characterize the subset of patients with long survival to better understand the complex biology and cancerogenic pathways of glioblastomas and, finally, to disclose better therapeutic design.

6. BIBLIOGRAPHY

1. Sung, H. et al. Global Cancer Statistics 2020: GLOBOCAN Estimates of Incidence and Mortality Worldwide for 36 Cancers in 185 Countries. CA Cancer J Clin, 71 (3): 209-249 (2021).

2. Ostrom, Q. T. et al. CBTRUS Statistical Report: Primary Brain and Other Central Nervous System Tumors Diagnosed in the United States in 2016-2020. Neuro Oncol, 25 (12 Suppl 2): iv1-iv99 (2023).

3. Associazione Italiana di Oncologia Medica (AIOM). I Numeri Del Cancro in Italia 2023 (2023).

4. Huang, J. et al. Disease burden, risk factors, and trends of primary central nervous system (CNS) cancer: A global study of registries data. Neuro Oncol, 25 (5): 995-1005 (2023).

5. Louis, D. N. et al. The 2016 World Health Organization Classification of Tumors of the Central Nervous System: a summary. Acta Neuropathol, 131 (6): 803-20 (2016).

6. Gritsch, S. et al. Diagnostic, therapeutic, and prognostic implications of the 2021 World Health Organization classification of tumors of the central nervous system. Cancer, 128 (1): 47-58 (2022).

7. Louis, D. N. et al. The 2021 WHO Classification of Tumors of the Central Nervous System: a summary. Neuro Oncol, 23 (8): 1231-1251 (2021).

8. Horbinski, C. et al. Clinical implications of the 2021 edition of the WHO classification of central nervous system tumours. Nat Rev Neurol, 18 (9): 515-529 (2022).

9. Pellerino, A. et al. Epidemiology, risk factors, and prognostic factors of gliomas. Clin Transl Imaging, 10 (12 Supp 2): 467–475 (2022).

10. Kinnersley, B. et al. Quantifying the heritability of glioma using genome-wide complex trait analysis. Sci Rep, 5: 17267 (2015).

11. Le Rhun, E. et al. Molecular targeted therapy of glioblastoma. Cancer Treat Rev, 80: 101896 (2019).

12. Wen, P.Y. et al. Glioblastoma in adults: a Society for Neuro-Oncology (SNO) and European Society of Neuro-Oncology (EANO) consensus review on current management and future directions. Neuro Oncol, 22 (8): 1073-1113 (2020).

13. D'Alessio, A. et al. Pathological and Molecular Features of Glioblastoma and Its Peritumoral Tissue. Cancers (Basel), 11 (4): 469 (2019).

14. Y. Shan, F. et al. Glioblastomas: Molecular Diagnosis and Pathology. IntechOpen, (2023).

15. Ramlal, B. et al. Gliomas, glioneuronal tumors and neuronal tumors - glioblastoma, IDH wild type. PathologyOutlines.com, (2024).

16. Ogawa, K. et al. Giant cell glioblastoma is a distinctive subtype of glioma characterized by vulnerability to DNA damage. Brain Tumor Pathol, 37 (1): 5-13 (2020).

17. Lowder, L. et al. Gliosarcoma: distinct molecular pathways and genomic alterations identified by DNA copy number/SNP microarray analysis. J Neurooncol, 143 (3): 381-392 (2019).

18. Yasin, I. et al. Gliomas, glioneuronal tumors and neuronal tumors, Other astrocytic tumors, Gliosarcoma. PathologyOutlines.com, (2024).

19. Miller, J. J. Targeting IDH-Mutant Glioma. Neurotherapeutics, 19 (6): 1724-1732, (2022).

20. Solomou, G. et al. Mutant IDH in Gliomas: Role in Cancer and Treatment Options. Cancers (Basel), 15 (11): 2883, (2023).

21. Cohen, A.L. et al. IDH1 and IDH2 mutations in gliomas. Curr Neurol Neurosci Rep, 13 (5): 345, (2013).

22. Christensen, B.C. et al. DNA methylation, isocitrate dehydrogenase mutation, and survival in glioma. J Natl Cancer Inst, 103 (2): 143-53, (2011).

23. Yang, H. et al. IDH1 and IDH2 mutations in tumorigenesis: mechanistic insights and clinical perspectives. Clin Cancer Res, 18 (20): 5562-71, (2012).

24. Zhang, Y. et al. The p53 Pathway in Glioblastoma. Cancers (Basel), 10 (9): 297, (2018).

25. England, B. et al. Current understanding of the role and targeting of tumor suppressor p53 in glioblastoma multiforme. Tumour Biol, 34 (4): 2063-74, (2013).

26. Qin, T. et al. ATRX loss in glioma results in dysregulation of cell-cycle phase transition and ATM inhibitor radio-sensitization. Cell Rep, 38 (2): 110216, (2022).

27. Gülten, G. et al. The importance of IDH1, ATRX and WT-1 mutations in glioblastoma. Pol J Pathol, 71 (2): 127-137, (2020).

28. Xie, Y. et al. Omics-based integrated analysis identified ATRX as a biomarker associated with glioma diagnosis and prognosis. Cancer Biol Med, 16 (4): 784-796, (2019).

29. Karsy, M. et al. New Molecular Considerations for Glioma: IDH, ATRX, BRAF, TERT, H3 K27M. Curr Neurol Neurosci Rep, 17 (2): 19, (2017).

30. Yu, W. et al. O6-Methylguanine-DNA Methyltransferase (MGMT): Challenges and New Opportunities in Glioma Chemotherapy. Front Oncol, sdx9: 1547, (2020).

31. Della Monica, R. et al. MGMT and Whole-Genome DNA Methylation Impacts on Diagnosis, Prognosis and Therapy of Glioblastoma Multiforme. Int J Mol Sci, 23 (13): 7148, (2022).

32. Liu, D. et al. Clinical strategies to manage adult glioblastoma patients without MGMT hypermethylation. J Cancer, 13 (1): 354-363 (2022).

33. Birzu, C. et al. Recurrent Glioblastoma: From Molecular Landscape to New Treatment Perspectives. Cancers (Basel), 13 (1): 47 (2020).

34. Powter, B. et al. Human TERT promoter mutations as a prognostic biomarker in glioma. J Cancer Res Clin Oncol, 147 (4): 1007-1017, (2021).

35. Olympios, N. et al. TERT Promoter Alterations in Glioblastoma: A Systematic Review. Cancers (Basel), 13 (5): 1147, (2021).

36. Śledzińska, P. Prognostic and Predictive Biomarkers in Gliomas. Int J Mol Sci, 22 (19): 10373 (2021).

37. Huang, L. E. Impact of CDKN2A/B Homozygous Deletion on the Prognosis and Biology of IDH-Mutant Glioma. Biomedicines, 10 (2): 246, (2022).

38. Funakoshi, Y. et al. Clinical significance of CDKN2A homozygous deletion in combination with methylated MGMT status for IDH-wildtype glioblastoma. Cancer Med, 10 (10): 3177-3187, (2021).

39. McNulty, S. N. et al. BRAF mutations may identify a clinically distinct subset of glioblastoma. Sci Rep, 11 (1): 19999, (2021).

40. Di Nunno, V. et al. Implications of BRAF V600E mutation in gliomas: Molecular considerations, prognostic value and treatment evolution. Front Oncol, 12: 1067252, (2023).

41. Han, F. et al. PTEN gene mutations correlate to poor prognosis in glioma patients: a meta-analysis. Onco Targets Ther, 9: 3485-92, (2016).

42. Yang, J. M. et al. Characterization of PTEN mutations in brain cancer reveals that pten mono-ubiquitination promotes protein stability and nuclear localization. Oncogene, 36 (26): 3673-3685, (2017).

43. Jimenez-Pascual, A. et al. Fibroblast Growth Factor Receptor Functions in Glioblastoma. Cells, 8 (7): 715, (2019).

44. Ardizzone, A. et al. Role of Fibroblast Growth Factors Receptors (FGFRs) in Brain Tumors, Focus on Astrocytoma and Glioblastoma. Cancers (Basel), 12 (12): 3825, (2020).

45. Rocha Pinheiro, S. L. et al. Immunotherapy in glioblastoma treatment: Current state and future prospects. World J Clin Oncol, 14 (4): 138-159, (2023).

46. Nabian, N. et al. State of the neoadjuvant therapy for glioblastoma multiforme-Where do we stand? Neurooncol Adv, 6 (1): vdae028, (2024).

47. Ghosh, M. et al. Survival and prognostic factors for glioblastoma multiforme: Retrospective single-institutional study. Indian J Cancer, 54 (1): 362-367, (2017).

48. Obrador, E. et al. Glioblastoma Therapy: Past, Present and Future. Int J Mol Sci, 25 (5): 2529, (2024).

49. Parsons, D. W. et al. , An integrated genomic analysis of human glioblastoma multiforme. Science, 321 (5897): 1807-12, (2008).

50. SongTao, Q. et al. IDH mutations predict longer survival and response to temozolomide in secondary glioblastoma. Cancer Sci, 103 (2): 269-73, (2012).

51. Szylberg, M. et al. MGMT Promoter Methylation as a Prognostic Factor in Primary Glioblastoma: A Single-Institution Observational Study. Biomedicines, 10 (8): 2030, (2022).

52. Jin MC, Wu A, Xiang M, Azad TD, Soltys SG, Li G, Pollom EL. Prognostic Factors and Treatment Patterns in the Management of Giant Cell Glioblastoma. World Neurosurg, 128: e217-e224, (2019).

53. Walid, M. S. Prognostic factors for long-term survival after glioblastoma. Perm J, 12 (4): 45-8 (2008).

54. Jovčevska, I. Genetic secrets of long-term glioblastoma survivors. Bosn J Basic Med Sci, 19 (2): 116-124, (2019).

55. Lim-Fat, M. J. et al. Clinical, radiological and genomic features and targeted therapy in BRAF V600E mutant adult glioblastoma. J Neurooncol, 152: 515–522, (2021).

56. Kalman, B. et al. Epidermal Growth Factor Receptor as a Therapeutic Target in Glioblastoma. Neuromol Med, 15: 420–434, (2013).

57. Xavier-Magalhães, A. et al. Nandhabalan M, Jones C, Costa BM. Molecular prognostic factors in glioblastoma: state of the art and future challenges. CNS Oncol, 2 (6): 495-510, (2013).

58. Miele, E. et al. Clinicopathological and molecular landscape of 5-year IDH-wild-type glioblastoma survivors: A multicentric retrospective study. Cancer Lett, 588: 216711, (2024).

59. Burgenske, D. M. et al. Molecular profiling of long-term IDH-wildtype glioblastoma survivors. Neuro Oncol, 21 (11): 1458-1469, (2019).